Table 1. DBZ is expressed exclusively in the brain as determined by northern blotting.

	Expression level (DBZ mRNA)
Brain	+++
Heart	-
Lung	-
Liver	-
Pancreas	-
Kidney	-
Muscle	-
Placenta	-

+++: Strong signal level; -: Weak signal level; DBZ: Disrupted-in-schizophrenia 1-binding zinc-finger protein.
Data from [14].

acids 348–597, participates in the interaction with DBZ (FIGURE 2). DBZ mRNA was expressed almost exclusively in the brain, but was not expressed in peripheral tissues (TABLE 1). Although overexpression of either DBZ or DISC1 alone had no effect, overexpression of both proteins resulted in a significant reduction in the number of neurite-bearing PC12 cells after PACAP stimulation, but not after NGF stimulation [14]. The region of DBZ encompassing amino acids 152–301 interacts with DISC1. We therefore used this fragment to examine the function of the DISC1–DBZ interaction. Expression of DBZ(152–301)–internal ribosome entry site–green fluorescent protein resulted in a significantly shorter neurite of PC12 cells treated with PACAP and rat primary culture hippocampal neurons, whereas DISC1–DBZ interaction did not affect the cell viability under our experimental conditions (FIGURE 3). PACAP stimulation increased both DISC1 and DBZ expression at 24 h after PACAP stimulation. These effects were inhibited by treatment with the PAC_1 receptor inhibitor. The co-immunoprecipitation of DISC1 with DBZ in lysates was reduced by approximately 80% at 1 h after treatment of PC12 cells with PACAP (100 nM). However, this reduction was transient and was followed by a gradual increase, with a return to the control level occurring by 24 h after PACAP treatment (FIGURE 4). Addition of an ERK inhibitor at 24 h after PACAP treatment resulted in the inhibition of rebinding of DBZ with DISC1, while an inhibitor of adenyl cyclase failed to influence the DISC1–DBZ binding, showing that PACAP regulates DISC1–DBZ binding through the ERK cascade but not through the cAMP cascade. The expression of DBZ is specific to the brain, and marked elevation of both DBZ and PAC_1 was observed during the perinatal stage.

Furthermore, downregulation of DBZ or DISC1 alone *in utero* causes a delay in the migration of cortical neurons [SATO M, UNIVERSITY OF FUKUI, FUKUI, JAPAN, PERS. COMM.]. These findings show that DBZ binds to DISC1 near the translocation breakpoint to cause the inhibition of neurite outgrowth; PACAP causes a marked but transient reduction in the association between DISC1 and DBZ in PC12 cells, and this reduction may induce the neurite extension; the effects of PACAP on the DISC1–DBZ interaction occur via the PAC_1 receptor and ERK pathway; and the DISC1–DBZ interaction plays a crucial role in brain development. During the dissociation, DISC1 might change the binding partner(s) participating in neurite growth. In brains in which translocation of DISC1 occurs, DBZ would be unable to bind to DISC1 and thus the dissociation between DISC1 and DBZ via PACAP that causes neurite extension may not be induced. However, another possibility should also be mentioned. Overexpression of DISC1 in PC12 cells induces the neurite extension, whereas downregulation of DISC1 expression inhibits the neurite outgrowth [10,16]. Moreover, PACAP stimulation also causes the neurite extension. Therefore, in the brain in which translocation of DISC1 occurs, it is likely that synergy of DISC1

Table 2. Comparison of mRNA between DISC1 and DBZ in the brain.

	DISC1	DBZ
Cortex	+	+++
Hippocampus	+	+++
Dentate gyrus	+++	+++
Thalamus	+	++
Substantia nigra	+	+
Olfactory bulb	+++	+
Cerebellum	++	+

Note that both DBZ and DISC1 mRNA are expressed in the hippocampus, and especially in the dentate gyrus.
+: Weak positive; ++: Strong; +++: Very strong; DBZ: DISC1-binding zinc-finger protein; DISC1: Disrupted-in-schizophrenia 1.
Data from [14].

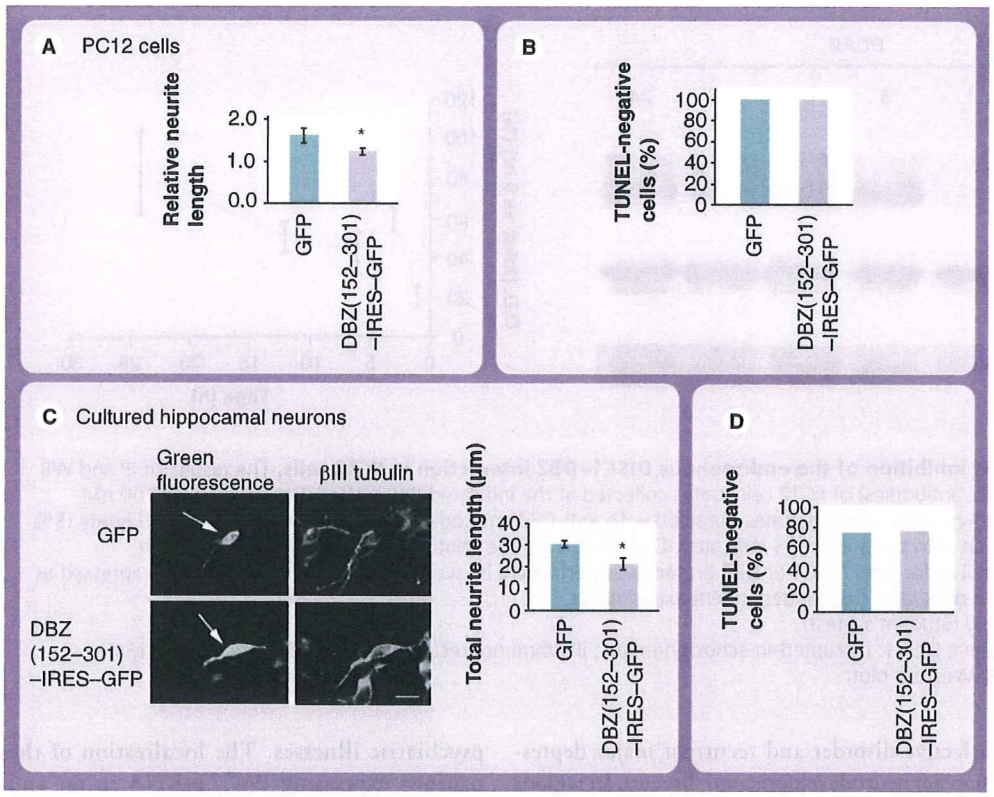

Figure 3. Neurite outgrowth was inhibited by the DISC1-binding domain of DBZ (DBZ[152–301]-IRES-GFP). (A) PC12 cells were transfected with DBZ(152–301)-IRES-GFP or GFP alone at 2 days after plating. After 24 h, cells were starved of serum for 4 h and treated with 100 nM PACAP for 48 h. Phase contrast and fluorescence microscopy images are shown. Diagrams are from three independent experiments. **(B)** GFP-positive cells were assessed for apoptosis by the TUNEL assay. Data are expressed as the mean ± standard error of mean of at least three independent experiments. **(C)** Rat hippocampal neurons were transiently transfected with DBZ(152–301)-IRES-GFP or the GFP expression vector. Cells were immunostained with anti-βIII-tubulin antibody at 24 h after transfection. Low power (left) and high-power (center) views of fluorescence microscopy images are shown. The diagrams show the total neurite length for transfected rat primary hippocampal neurons (right). Approximately 50 cells were randomly counted in three independent experiments. **(A,C)** Arrows indicate GFP-positive transfected cells. *$p < 0.05$ (Student's *t*-test). Scale bars = 20 μm. **(D)** GFP-positive cells were assessed for apoptosis by the TUNEL assay. Data are expressed as the means ± standard error of mean of at least three independent experiments.
DBZ: DISC1-binding zinc-finger protein; GFP: Green fluorescent protein; IRES: Internal ribosome entry site; PACAP: Pituitary adenylate cyclase-activating polypeptide; TUNEL: Terminal deoxynucleotidyl transferase-dUTP nick end labeling.
Adapted from [14].

and PACAP function causes the hyperplasia of neurites, though direct evidence demonstrating this is lacking at present.

DISC1-binding zinc-finger protein may provide a link between DISC1 and PACAP signaling in granule cells of the dentate gyrus *in vivo*. In rats, the overlapping areas that exhibit both DISC1 and DBZ expression are the hippocampus, olfactory tubercle, cerebral cortex and striatum. In addition, co-expression of DBZ and PAC$_1$ mRNA is detected in the granule cells of the dentate gyrus, where a high level of *DISC1* mRNA expression was also observed in both young and adult rat brains. PACAP is localized in the entorhinal cortex neurons and perforating fibers, and PAC$_1$ protein is localized in hippocampal mossy fiber terminals [48]. Therefore, regulation by PACAP of the association between DISC1 and DBZ may occur at the synapse between PACAP-containing perforating fibers and PAC$_1$-expressing mossy fibers (Figure 5).

As mentioned above, PACAP dissociates the binding between DISC1 and DBZ to cause neurite outgrowth in the granular cells in the dentate gyrus, and development of the granular cells may be inhibited in the DISC1-translocated brain, suggesting that schizophrenia, bipolar

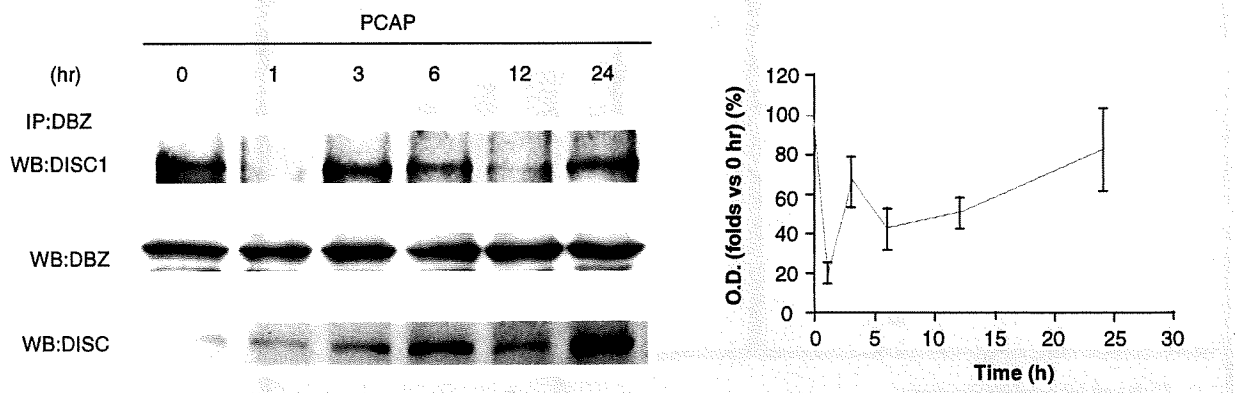

Figure 4. PACAP causes transient inhibition of the endogenous DISC1–DBZ interaction in PC12 cells. The results of IP and WB analysis (with anti-DISC1 or anti-DBZ antibodies) of PC12 cell lysates collected at the indicated times after stimulation with 100 nM PACAP by the same method are shown. Immunoprecipitates obtained with anti-DBZ antibodies (DBZ), as well as 5% of each lysate (5% input), were subjected to WB analysis with the antibodies indicated. Quantitation of the relative band densities for DISC1 co-immunoprecipitated with DBZ as well as for total DISC1 or DBZ protein was performed by scanning densitometry. Data are expressed as the means ± standard error of mean of at least three independent experiments.
*$p < 0.05$ versus the control at time 0 (Student's *t*-test).
DBZ: DISC1-binding zinc-finger protein; DISC1: Disrupted-in-schizophrenia 1; IP: Immunoprecipitation; PACAP: Pituitary adenylate cyclase-activating polypeptide; WB: Western blot.
Adapted from [14].

affective disorder and recurrent major depression are neurodevelopmental diseases. In regions other than the dentate gyrus, DBZ has also been shown to play a role in cerebral neurogenesis. Knock-down of DBZ causes a delay in the migration of cortical neurons, and administration of DBZ reverses this delay [Sato M, University of Fukui, Fukui, Japan, Pers. Comm.].

Molecular mechanism of PACAP deficiency-induced psychiatric illnesses

PACAP–PAC_1–DBZ system

In PACAP-knock out (KO) mice and PAC_1-KO mice, the PACAP signal is not transmitted from the presynaptic site to the postsynaptic element. Therefore, in these animals, dissociation between DISC1 and DBZ is not induced, and thus the neurite extension of the granular cells of the dentate gyrus is inhibited. PACAP deficiency-induced psychiatric illnesses might be attributed to a dysfunction of the dissociation of the DISC1–DBZ interaction, though the possibility that other downstream pathways not involving the DISC1–DBZ interaction could account for abnormalities seen in these mice could not be excluded. At present, there are no reports showing the association of DISC1 and DBZ SNPs with psychiatric illness.

PACAP–stathmin1 cascade

However, little is known in regard to the mechanism of PACAP deficiency-induced psychiatric illnesses. The localization of the neurons expressing PAC_1 mRNA in rat and mouse brains has been examined by *in situ* hybridization histochemistry [48]. Neurons expressing intense signals for PAC_1 mRNA were found in the olfactory bulb, dentate gyrus of the hippocampus, second layer of the cerebral cortex and several hypothalamic areas in these species. In addition, cytoarchitectural change in the hippocampus has been reported in schizophrenia [49–51]. Thus, the overlapping area that expresses PAC_1 and is related to schizophrenia is the dentate gyrus. In addition, as described above, granular cells in the dentate gyrus receive the PACAP-containing inputs from the entorhinal cortex as perforating fibers. Therefore, in order to clarify the molecular mechanism of PACAP-dependent psychiatric disorders, we have first attempted to isolate the PACAP deficiency-regulated gene in the dentate gyrus of the mice using a differential display method, because the overlapping area that expresses PAC_1 and is related to schizophrenia is the dentate gyrus. Expression of stathmin1 is upregulated in the dentate gyrus both at the mRNA and protein levels [52]. In addition, PACAP stimulation inhibits the stathmin1 expression in PC12 cells. Subsequent analysis by means of *in situ* hybridization histochemistry and immunohistochemistry showed that stathmin1 is upregulated in the subgranular zone (SGZ) neurons (Figure 6A & B). In addition, we have found that increased expression of stathmin1

in the neurons of the SGZ and primary cultured neurons from the hippocampus induces the abnormal arborization of the processes both *in vivo* and *in vitro* (FIGURE 6C, D, F & G). An *in vivo* analysis demonstrated that they are distributed in the hilus (FIGURE 6C & D), while analysis by immunoelectron microscopy demonstrated that the sprouting processes are axons. In support of these findings, several previous studies have shown that stathmin1 plays a neurodevelopmental role in the brain. A previous report showed that stathmin1 is required for the induction of LTP in afferent inputs to the amygdala and is essential in regulating both innate and learned fear [53]. Cardinaux *et al.* reported that brain-derived neurotrophic factor stimulates the phosphorylation of stathmin1 [54]. Rowlands *et al.* showed that stathmin1 is expressed in the proliferating cells, while nonproliferating cells do not express stathmin1 [55]. These findings suggest that stathmin1 plays an important role in brain development. In the future, in order to establish that abnormal ramification of neurites caused by an increase of stathmin1 expression is involved in the abnormal behavioral phenotype of PACAP-KO and PAC$_1$-KO mice, it would be useful to examine whether or not stathmin1 transgenic mice exhibit a phenotype similar to PACAP-KO or PAC$_1$-KO mice. In our previous study, we also posited the following molecular mechanism by which PACAP may regulate stathmin1 expression [52]. PACAP stimulation

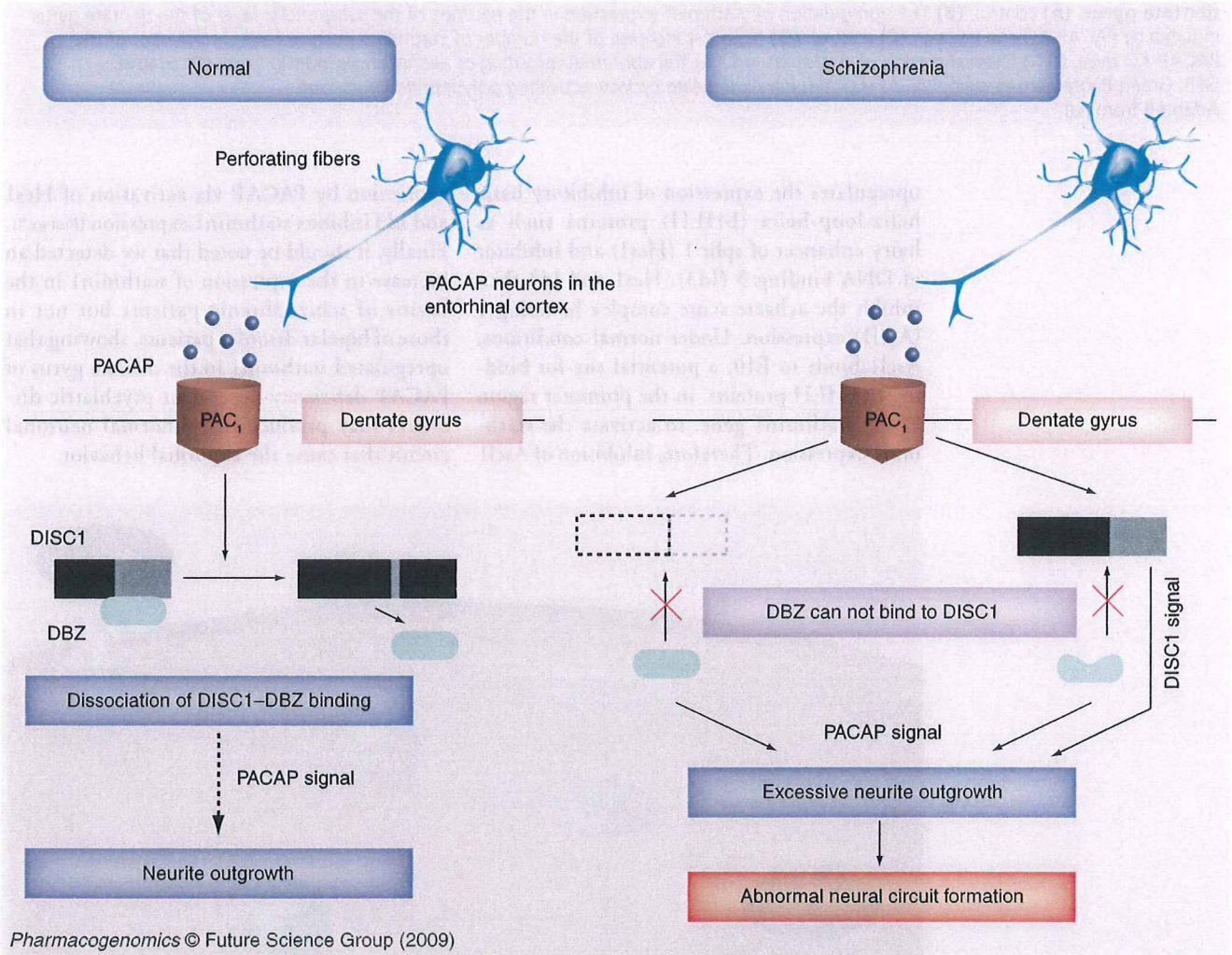

Pharmacogenomics © Future Science Group (2009)

Figure 5. A possible PACAP-containing pathway related to regulation of the DISC1–DBZ interaction. In the normal side PACAP leads to temporal dissociation of DISC1 and DBZ binding, which in turn leads to normal neurite outgrowth. On the schizophrenia side, illustrated by DISC1 either being truncated or absent completely, DISC1–DBZ binding does not occur (left pathway in schizophrenia side). In this case, the PACAP signal may proceed without inhibition. If DBZ mutation occurs, DISC1–DBZ binding does not occur (right pathway in schizophrenia side). In this case, neurite outgrowth may proceed excessively not only from the PACAP signal but also the DISC1 signal. DBZ: DISC1-binding zinc-finger protein; DISC1: Disrupted-in-schizophrenia 1; PACAP: Pituitary adenylate cyclase-activating polypeptide.

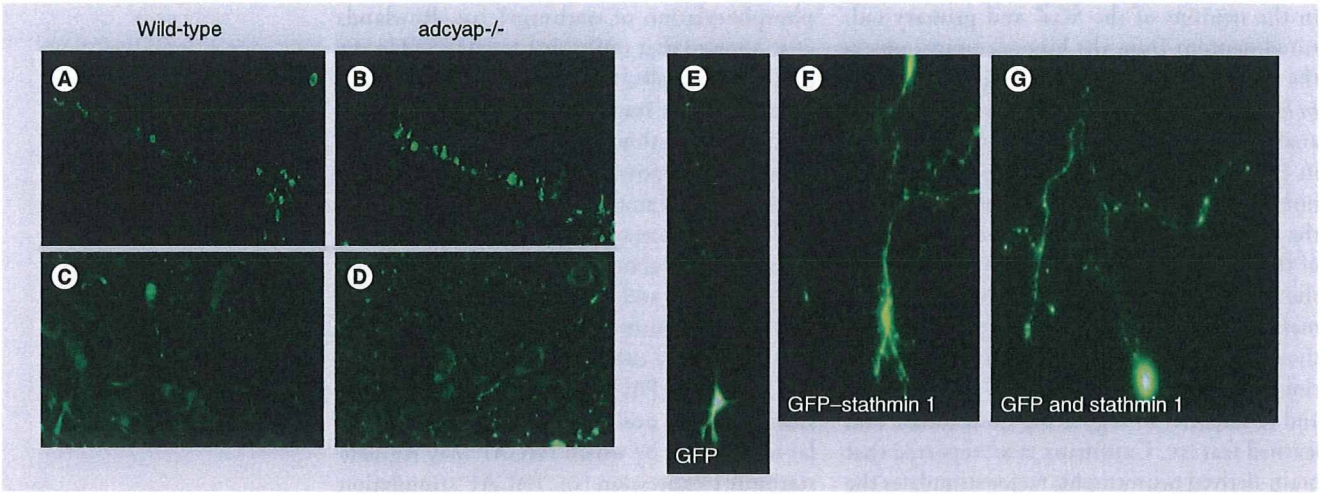

Figure 6. PACAP-KO induces the upregulation of stathmin1 expression in the neurons of the subgranular layer of the dentate gyrus. (A) control. **(B)** The upregulation of stathmin1 expression in the neurons of the subgranular layer of the dentate gyrus induced by PACAP-KO can be seen **(C)** control. **(D)** Note the increase of the number of stathmin1 positive fibers in the hilus of the PACAP-KO mice. **(F,G)** Overexpression of stathmin1 induces the abnormal sprouting of axonal fibers in PC12 cells. **(E)** control.
GFP: Green fluorescent protein; PACAP-KO: Pituitary adenylate cyclase-activating polypeptide knock out.
Adapted from [52].

upregulates the expression of inhibitory basic helix-loop-helix (bHLH) proteins such as hairy enhancer of split 1 (Hes1) and inhibitor of DNA binding 3 (Id3). Hes1 and Id3 then inhibit the achaete scute complex homolog 1 (Ascl1) expression. Under normal conditions, Ascl1 binds to E10, a potential site for binding to bHLH proteins, in the promoter region of the stathmin1 gene, to activate the stathmin1 expression. Therefore, inhibition of Ascl1 expression by PACAP via activation of Hes1 and Id3 inhibits stathmin1 expression (FIGURE 7). Finally, it should be noted that we detected an increase in the expression of stathmin1 in the brains of schizophrenic patients but not in those of bipolar disorder patients, showing that upregulated stathmin1 in the dentate gyrus of PACAP deficiency-dependent psychiatric disorders may produce the abnormal neuronal circuit that cause the abnormal behavior.

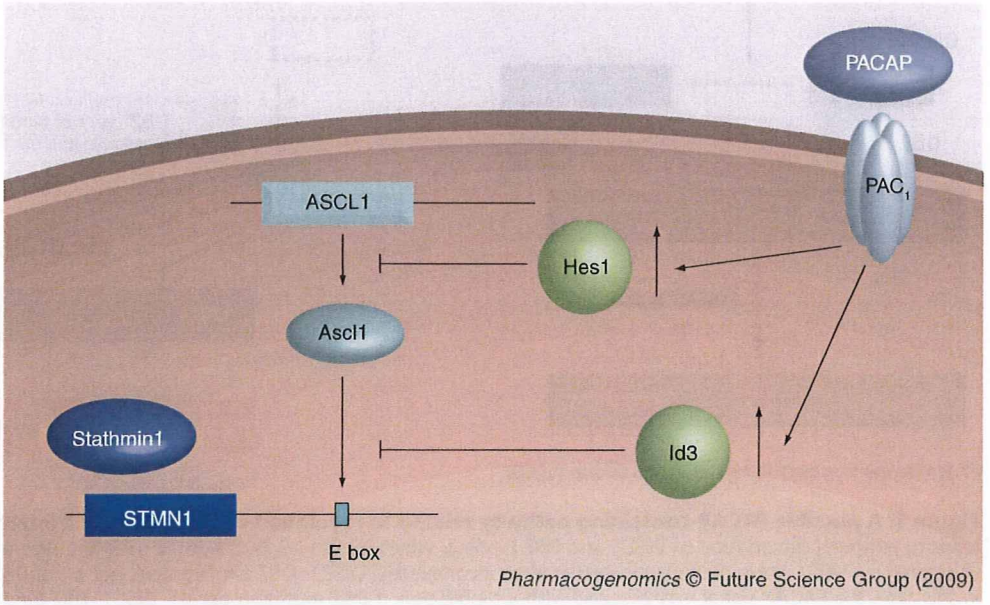

Figure 7. Molecular cascade of the inhibition of stathmin1 expression by PACAP.
PACAP-KO: Pituitary adenylate cyclase-activating polypeptide.

Pathogenesis of schizophrenia caused by DISC1–DBZ & PACAP–stathmin1 might be different, even though both systems are involved in neuronal development

As shown above, dissociation between DISC1 and DBZ by PACAP induces the neurite outgrowth. Therefore, in the brain in which translocation of DISC1 occurs, dissociation between DISC1 and DBZ via PACAP may not be induced, because DBZ cannot bind to DISC1. PACAP-KO induces the upregulation of stathmin1 in SGZ neurons. Overexpression of stathmin1 in the cultured neuronal cells induced remarkably advanced arborization of processes from stem neurites, though the effects of stathmin1 on the length of neurites could not be clearly identified. These findings show that dysfunction of the DISC1–DBZ system causes the inhibition of neurite extension, while PACAP deficiency induces the abnormal ramification of branches of neurites, suggesting a multiplex pathogenesis of schizophrenia according to the different molecules.

Conclusion & future perspective: possible novel treatment utilizing PACAP–DISC1/DBZ/FEZ1 or the PACAP–stathmin1 pathway

Are NGF & PACAP new candidate molecules for the treatment of schizophrenia & bipolar disease?

It is unclear why the disruption of DISC1 by translocation selectively causes psychiatric diseases despite the fact that DISC1 is ubiquitously expressed throughout the whole body. DISC1 has been proposed to be a multifunctional protein that interacts with multiple proteins of the centrosome and cytoskeletal system at distinct domains such as Nudel, FEZ1, pericentrin B and DBZ. The latter three proteins bind to an area near the breakpoint of DISC1. The expression of FEZ1 is highly specific to the brain, and that of DBZ is somewhat specific to the brain. We have revealed that both the DISC1–FEZ1 interaction and the DISC1–DBZ interaction play a crucial role in the development of the mammalian nervous system. This raises the possibility that dysfunction of DISC1 may lead to abnormal development of the nervous system, and thereby susceptibility to psychiatric illness. We further demonstrated that NGF upregulates the DISC1–FEZ1 interaction and PACAP induces the transient dissociation of the DISC1–DBZ interaction. In individuals carrying the chromosomal translocation that segregates mental diseases, the truncated mutant DISC1 protein would be produced or the expression of DISC1 protein would be reduced. In the case of truncated mutant protein expression, FEZ1 and DBZ would not be able to interact with DISC1. Loss of DISC1 protein expression could lead to neurite outgrowth by disrupting the DISC1–FEZ1 and DISC1–DBZ interaction. If DISC1 expression is reduced, and only a small amount of DISC1 is produced in the carrier of the chromosomal translocation of DISC1, NGF and PACAP could have potential as a novel treatment for schizophrenia or bipolar disease caused by dysfunction of DISC1, because both NGF and PACAP upregulate DISC1 expression. From this point of view, agonists of the PAC_1 receptor or NGF receptors are also possible candidates. However, there are many high hurdles to be cleared before realizing such treatments, such as examination of the effects of NGF or PACAP on model animals. In addition, such treatments could cause a wide range of side effects, since NGF, PACAP, PAC_1 and NGF receptors are widely and abundantly distributed throughout the entire body.

Is regulation of PACAP/stathmin1 function a new target for the treatment of schizophrenia or bipolar disease?

In PACAP-KO mice, expression of stathmin1 is increased, causing an abnormal arborization of axonal fibers of SGZ neurons in the dentate gyrus. In addition, stathmin1 expression is upregulated in the brains of schizophrenic patients but not in the brains of patients with bipolar disease, showing that dysfunction of the PACAP-stathmin1 pathway is specifically related to schizophrenia. In addition, stathmin1 is expressed preferentially in the brain. Therefore, control of stathmin1 expression is a good target for treatment of schizophrenia: toward this end, a range of investigations are needed, including promoter analysis of the stathmin1 gene to search for molecules that could downregulate stathmin1 expression. In addition, it will be important to identify molecules that belong to the inhibitory bHLH family and localize specifically in the brain, because these molecules inhibit stathmin1 expression.

Financial & competing interests disclosure

The authors have no relevant affiliations or financial involvement with any organization or entity with a financial interest in or financial conflict with the subject matter or materials discussed in the manuscript. This includes employment, consultancies, honoraria, stock ownership or options, expert testimony, grants or patents received or pending, or royalties.

No writing assistance was utilized in the production of this manuscript.

Executive summary

Disrupted-in-schizophrenia 1 (DISC1) binds to different molecules at various intracellular sites, revealing its multifunctional nature

- *DISC1* has been identified as a potential susceptibility gene for major psychiatric disorders.
- Disruption of this gene by a balanced (1;11)(q42.1;q14.3) translocation results in a predicted C-terminal truncation of the open reading frame, and this anomaly has been associated with schizophrenia, bipolar affective disorder and recurrent major depression in a large Scottish family.
- DISC1 binds to fasciculation and elongation protein zeta-1 (FEZ1), pericentrin B (kendrin), DISC1-binding zinc-finger protein (DBZ), NUDEL and lissencehphaly-1 (LIS1). The former three proteins bind to the regions near the translocation site.
- Interactions between DISC1 and FEZ1; DISC1 and DBZ; and DISC1 and pericentrin B are involved in neural development.

Pituitary adenylate cyclase-activating polypeptide (PACAP) regulates the DISC1/DBZ interaction: a new mechanism that contributes to psychiatric disorders

- PACAP markedly and transiently reduces the association between DISC1 and DBZ in PC12 cells, which in turn may induce the neurite extension.
- The effects of PACAP on the DISC1–DBZ interaction occur via the PAC_1 receptor and the ERK pathway.
- DISC1–DBZ interaction plays a crucial role in brain development.
- DBZ may provide a link between DISC1 and PACAP signaling in granule cells of the dentate gyrus *in vivo*.
- PACAP knock-out mice exhibited prominent behavioral abnormalities that included hyperactivity with impaired habituation to novel situations, increased novelty-seeking behavior and reduced anxiety, as well as evidence of neuronal dysfunction, such as impairment of prepulse inhibition and hippocampal long-term potentiation.
- PAC_1 receptor (PAC_1)-deficient mice also demonstrated an increase in locomotor activity, reduced anxiety-like behavior and abnormal social behavior, as well as impairment of hippocampal long-term potentiation.
- Some SNPs of the *PACAP* gene have an association with schizophrenia.

Molecular mechanism of PACAP deficiency-induced psychiatric illnesses

- PACAP deficiency-induced psychiatric illnesses could be attributed to a dysfunction of the DISC1–DBZ interaction.
- PACAP deficiency induces upregulation of stathmin1 in the subgranular zone of the dentate gyrus.
- Overexpression of stathmin1 induces abnormal sprouting of the axon fibers both *in vivo* and *in vitro*.
- Stathmin1 gene promoter activity is regulated by the basic helix-loop-helix protein.

Conclusion & future perspective

- PACAP is a new candidate molecule for treatment of schizophrenia and bipolar disease.
- Regulation of PACAP/stathmin1 function may be a new target for treatment of schizophrenia or bipolar disease.

Bibliography

Papers of special note have been highlighted as:
* of interest
** of considerable interest

1 Weinberger DR: Implications of normal brain development for the pathogenesis of schizophrenia. *Arch. Gen. Psychiatry* 44, 660–669 (1987).

2 Lewis DA, Lieberman JA: Catching up on schizophrenia: natural history and neurobiology. *Neuron* 28, 325–334 (2000).

3 Frankle WG, Lerma J, Laruelle M: The synaptic hypothesis of schizophrenia. *Neuron* 39, 205–216 (2003).

4 Heinz A, Romero B, Gallinat J *et al.*: Molecular brain imaging and the neurobiology and genetics of schizophrenia. *Pharmacopsychiatry* 36, S152–S157 (2003).

5 Mueser KT, McGurk SR: Schizophrenia. *Lancet* 363, 2063–2072 (2004).

6 Harrison PJ, Weinberger DR: Schizophrenia genes, gene expression, and neuropathology: on the matter of their convergence. *Mol. Psychiatry* 10, 40–60 (2005).

7 Millar JK, Wilson-Annan JC, Anderson S *et al.*: Distribution of two novel genes by a translocation co-segregating with schizophrenia. *Hum. Mol. Genet.* 9, 1415–1423 (2000).

8 Millar JK, Christie S, Anderson S *et al.*: Genomic structure and localization within a linkage hotspot of disrupted in schizophrenia 1, a gene disrupted by a translocation segregating with schizophrenia. *Mol. Psychiatry* 6, 173–178 (2001).

9 Sachs NA, Sawa A, Holmes SE *et al.*: A frameshift mutation in disrupted in schizophrenia 1 in an American family with schizophrenia, schizoaffective disorder. *Mol. Psychiatry* 10, 758–764 (2005).

10 Miyoshi K, Honda A, Baba K *et al.*: Disrupted-in-schizophrenia 1, a candidate gene for schizophrenia, participates in neurite outgrowth. *Mol. Psychiatry* 8, 685–694 (2003).

* **First study to report that the interaction of disrupted-in-schizophrenia 1 (DISC1) with FEZ1 is involved in neurite outgrowth.**

11 Honda A, Miyoshi K, Baba K *et al.*: Expression of fasciculation and elongation protein zeta-1 (FEZ1) in the developing rat brain. *Brain Res. Mol. Brain Res.* 122, 89–92 (2004).

12 Miyoshi K, Asanuma M, Miyazaki I *et al.*: DISC1 localizes to the centrosome by binding to kendrin. *Biochem. Biophys. Res. Commun.* 317, 1195–1199 (2004).

* **First study to report that kendrin interacts with DISC1.**

13 Shimizu S, Matsuzaki S, Hattori T *et al.*: DISC1-kendrin interaction is involved in centrosomal microtubule network formation. *Biochem. Biophys. Res. Commun.* 377, 1051–1056 (2008).

14 Hattori T, Baba K, Matsuzaki S *et al.*: A novel DISC1-interacting partner DISC1-binding zinc finger protein: implication in the modulation of DISC1-dependent neurite outgrowth *Mol. Psychiatry* 12, 398–407 (2007).

** **First study to report that interaction between DISC1 and DISC1-binding zinc-finger protein (DBZ) is regulated by pituitary adenylate cyclase-activating polypeptide (PACAP), which affects neurite outgrowth.**

15 Kuroda S, Nakagawa N, Tokunaga G *et al.*: Mammalian homologue of the *Caenorhabditis elegans* UNC-76 protein involved in axonal outgrowth is a protein kinase C zeta-interacting protein. *J. Cell Biol.* 144, 403–411 (1999).

16 Duan X, Chang JH, Ge S *et al.*: Disrupted-In-Schizophrenia 1 regulates integration of newly generated neurons in the adult brain. *Cell* 130(6), 1146–1158 (2007).

17 Millar JK, Pickard BS, Mackie S *et al.*: *DISC1* and *PDE4B* are interacting genetic factors in schizophrenia that regulate cAMP signaling. *Science* 310(5751), 1187–1191 (2005).

18 Yamada K, Nakamura K, Minabe Y *et al.*: Association analysis of *FEZ1* variants with schizophrenia in Japanese cohorts. *Biol. Psychiatry* 56, 683–690 (2004).

19 Hashimoto R, Hashimoto H, Shintani N *et al.*: Pituitary adenylate cyclase-activating polypeptide is associated with schizophrenia. *Mol. Psychiatry* 12, 1026–1032 (2007).

20 Anitha A, Nakamura K, Yamada Y *et al.*: Gene and expression analysis reveal enhanced expression of pericentrin 2 (PCNT2) in bipolar disorder. *Biol. Psychiatry* 63, 678–685 (2008).

* **Study that suggests a potential association between elevated levels of PCNT2 and clinical outcome in bipolar disorder patients.**

21 Anitha A, Nakamura K, Yamada K *et al.*: Association studies and gene expression analyses of the DISC1-interacting molecules, pericentrin 2 (PCNT2) and DISC1-binding zinc finger protein (DBZ), with schizophrenia and with bipolar disorder. *Am. J. Med. Genet. B. Neuropsychiatr. Genet.* 150B(7), 967–976 (2009).

22 Numata S, Iga J, Nakataki M *et al.*: Positive association of the pericentrin (*PCNT*) gene with major depressive disorder in the Japanese population. *J. Psychiatry Neurosci.* 34(3), 195–198 (2009).

23 Hodgkinson CA, Goldman D, Ducci F *et al.*: The *FEZ1* gene shows no association to schizophrenia in Caucasian or African American populations. *Neuropsychopharmacology* 32(1), 190–196 (2007).

24 Koga M, Ishiguro H, Horiuchi Y *et al.*: Failure to confirm the association between the *FEZ1* gene and schizophrenia in a Japanese population. *Neurosci. Lett.* 417(3), 326–329 (2007).

25 Ishiguro H, Ohtsuki T, Okubo Y *et al.*: Association analysis of the pituitary adenyl cyclase activating peptide gene (*PACAP*) on chromosome 18p11 with schizophrenia and bipolar disorders. *J. Neural. Transm.* 108(7), 849–854 (2001).

26 Millar JK, Christie S, Porteous DJ: Yeast two-hybrid screens implicate DISC1 in brain development and function. *Biochem. Biophys. Res. Commun.* 311, 1019–1025 (2003).

27 Morris JA, Kandpal G, Ma L *et al.*: DISC1 (Disrupted-In-Schizophrenia 1) is a centrosome-associated protein that interacts with MAP1A, MIPT3, ATF4/5 and Nudel: regulation and loss of interaction with mutation. *Hum. Mol. Genet.* 12, 1591–1608 (2003).

28 Ozeki, Y, Tomoda T, Kleiderlein J *et al.*: Disrupted-in-Schizophrenia-1 (DISC-1): mutant truncation prevents binding to Nude-like (NUDEL) and inhibits neurite outgrowth. *Proc. Natl Acad. Sci. USA* 100, 289–294 (2003).

29 Brandon NJ, Handford EJ, Schurov I *et al.*: Disrupted in Schizophrenia 1 and Nudel form a neurodevelopmentally regulated protein complex: implications for schizopherenia and other major neurological disorders. *Mol. Cell Neurosci.* 25, 42–55 (2004).

30 Chubb JE, Bradshaw NJ, Soare DC *et al.*: The DISC1 locus in psychiatric illness. *Mol. Psychiatry* 13, 36–64 (2008).

31 Ikeda M, Hikita T, Taya S *et al.*: Identification of YWHAE, a gene encoding 14–13–3ε, as a possible susceptibility gene for schizophrenia. *Hum. Mol. Genet.* 17(20), 3212–3222 (2008).

32 Mao Y, Ge X, Frank CL *et al.*: Disrupted in schizophrenia 1 regulates neuronal progenitor proliferation via modulation of GSK3β/β-catenin signaling. *Cell* 136, 1017–1031 (2009).

33 Niethammer M, Smith DS, Ayala R *et al.*: Nudel is a novel Cdk5 substrate that associates with LIS1 and cytoplasmic dynein. *Cell* 28, 697–711 (2000).

34 Sasaki S, Shinoyama A, Ishida M *et al.*: A LIS1/NUDLE/cytoplasmic dynein heavy chain complex in the developing and adult nervous system. *Neuron* 28, 681–696 (2000).

35 Shu T, Ayala R, Nguyen MD *et al.*: Nudel1 operates in a common pathway with LIS1 and cytoplasmic dynein to regulate cortical neuronal positioning. *Neuron* 44, 263–277 (2004).

36 Tanaka T, Serno FF, Higgins C *et al.*: Lis1 and double cortin function with dynein to mediate coupling of the nucleus to the centrosome in neuronal migration. *J. Cell Biol.* 165, 709–721 (2004).

37 Kamiya A, Kubo K, Tomoda T *et al.*: A schizophrenia-associated mutation of DISC1 perturbs cerebral cortex development. *Nat. Cell Biol.* 7, 1067–1078 (2005).

** **First study to report that DISC1 has a important role in cerebral cortex formation.**

38 Shinoda T, Taya S, Tsuboi D *et al.*: DISC1 regulates neurotrophin-induced axon elongation via interaction with Grb2. *J. Neurosci.* 27, 4–14 (2007).

39 Taya S, Shinoda D, Tsuboi D *et al.*: DISC1 regulates the transport of the NUDEL/LIS1/14–13–3epsin complex through kinesin-1. *J. Neurosci.* 27, 15–26 (2007).

40 Arimura A: Perspectives on pituitary adenylate cyclase activating polypeptide (PACAP) in the neuroendocrine, endocrine, and nervous system. *Jpn. J. Physiol.* 48, 301–331 (1998).

41 Vaudry D, Gonzalez BJ, Basille M, Yon L, Fournier A, Vaudry H: Pituitary adenylate cyclase-activating polypeptide and its receptors: from structure to functions. *Pharmacol. Rev.* 52, 269–324 (2000).

42 Hashimoto H, Shintani N, Tanaka K *et al.*: Altered psychomotor behaviors in mice lacking pituitary adenylate cyclase-activating polypeptide (PACAP). *Proc. Natl Acad. Sci. USA* 98, 13355–13360 (2001).

** **First study to report that PACAP-deficient mice display remarkable behavioral abnormalities.**

43 Tanaka K, Shintani N, Hashimoto H *et al.*: Psychostimulant-induced attenuation of hyperactivity and prepulse inhibition deficits in Adcyap1-deficient mice. *J. Neurosci.* 26(19), 5091–5097 (2006).

44 Matsuyama S, Matsumoto A, Hashimoto H *et al.*: Impaired long term potentiation *in vivo* in the dentate gyrus of pituitary adenylate cyclase-activating polypeptide (PACAP) or PACAP type 1 receptor-mutant mice. *Neuroreport* 14, 2095–2098 (2003).

45 Matsuyama S, Matsumoto A, Hashimoto H, Shintani N, Baba A: Impairment of mossy fiber long-term potentiation and associative learning in pituitary adenylate cyclase activating polypeptide type I receptor-deficient mice. *J. Neurosci.* 21, 5520–5527 (2001).

46 Otto C, Martin M, Wolfer DP *et al.*: Altered emotional behavior in PACAP-type-I-receptor-deficient mice. *Brain Res. Mol. Brain Res.* 92, 78–84 (2001).

* **First study to report that PAC_1-receptor deficient mice have been demonstrated to exhibit elevated locomotor activity and reduced anxiety-like behavior.**

47 Nicot A, Otto T, Brabet P *et al.*: Altered social behavior in pituitary adenylate cyclase-activating polypeptide type I receptor-deficient mice. *J. Neurosci.* 24, 8786–8795 (2004).

48 Hashimoto H, Nogi H, Mori K *et al.*: Distribution of the mRNA for a pituitary adenylate cyclase-activating polypeptide receptor in the rat brain: an *in situ* hybridization study. *J. Comp. Neurol.* 377, 567–577 (1996).

49 Harrison PJ: The neuropathology of schizophrenia. A critical review of the data and their interpretation. *Brain* 122, 593–624 (1999).

50 Heckers S, Konradi C: Hippocampal neurons in schizophrenia. *J. Neural Transm.* 109, 891–905 (2002).

51 Harrison PJ, Eastwood SL: Neuropathological studies of synaptic connectivity in the hippocampal formation in schizophrenia. *Hippocampus* 11, 508–519 (2001).

52 Yamada K, Matsuzaki S, Hattori T *et al.*: Increased stathmin 1 expression in the dentate gyrus causes abnormal axonal arborizations potential relevance to schizophrenia. *PLoS ONE* (2009) (In press).

53 Shumyatsky GP, Malleret G, Shin RM *et al.*: Stathmin, a gene enriched in the amygdala, controls both learned and innate fear. *Cell* 123(4), 697–709 (2005).

* **First study to report that stathmin1 deficient mice exhibit decreased memory in amygdala-dependent fear conditioning and fail to recognize danger in innately aversive environments.**

54 Cardinaux JR, Magistretti PJ, Martin JL: Brain-derived neurotrophic factor stimulates phosphorylation of stathmin in cortical neurons. *Mol. Brain Res.* 51, 220–228 (1997).

55 Rowlands DC, Williams A, Jones NA *et al.*: Stathmin expression is a feature of proliferating cells of most, if not all, cell lineages. *Lab. Invest.* 72, 100–113 (1995).

The FASEB Journal • Research Communication

Pericentrin, a centrosomal protein related to microcephalic primordial dwarfism, is required for olfactory cilia assembly in mice

Ko Miyoshi,*[,1] Kyosuke Kasahara,* Ikuko Miyazaki,* Shoko Shimizu,[†] Manabu Taniguchi,[†] Shinsuke Matsuzaki,[†,‡] Masaya Tohyama,[†,‡] and Masato Asanuma*

*Department of Brain Science, Graduate School of Medicine, Dentistry and Pharmaceutical Sciences, Okayama University, Okayama, Japan; and [†]Department of Anatomy and Neuroscience and [‡]The Osaka-Hamamatsu Joint Research Center for Child Mental Development, Graduate School of Medicine, Osaka University, Osaka, Japan

ABSTRACT **The *Drosophila* pericentrin-like protein has been shown to be essential for the formation of the sensory cilia of chemosensory and mechanosensory neurons by mutant analysis in flies, while the *in vivo* function of pericentrin, a well-studied mammalian centrosomal protein related to microcephalic primordial dwarfism, has been unclear. To determine whether pericentrin is required for ciliogenesis in mammals, we generated and analyzed mice with a hypomorphic mutation of *Pcnt* encoding the mouse pericentrin. Immunofluorescence analysis demonstrated that olfactory cilia of chemosensory neurons in the nasal olfactory epithelium were malformed in the homozygous mutant mice. On the other hand, the assembly of motile and primary cilia of non-neuronal epithelial cells and the formation of sperm flagella were not affected in the *Pcnt*-mutant mice. The defective assembly of olfactory cilia in the mutant was apparent from birth. The mutant animals displayed reduced olfactory performance in agreement with the compromised assembly of olfactory cilia. Our findings suggest that pericentrin is essential for the assembly of chemosensory cilia of olfactory receptor neurons, but it is not globally required for cilia formation in mammals.—Miyoshi, K., Kasahara, K., Miyazaki, I., Shimizu, S., Taniguchi, M., Matsuzaki, S., Tohyama, M., Asanuma, M. Pericentrin, a centrosomal protein related to microcephalic primordial dwarfism, is required for olfactory cilia assembly in mice. *FASEB J.* 23, 3289–3297 (2009). www.fasebj.org**

Key Words: kendrin · ciliogenesis · olfaction

PERICENTRIN (PCNT), ALSO referred to as kendrin, and CG-NAP, also referred to as AKAP350 or AKAP450, are mammalian centrosomal proteins with partial amino acid-sequence homology (1–4). These two giant proteins share a pericentrin/AKAP450 centrosomal targeting (PACT) domain in their C termini (5) and have been implicated in recruiting several proteins to the centrosome (6, 7). It has been reported that mitosis-specific anchoring of the γ-tubulin complex to the centrosome by Pcnt controls the organization of the mitotic spindle, a highly dynamic structure composed of microtubules (8). In flies, the *Drosophila* pericentrin-like protein (D-PLP) has been found as the only PACT domain-containing protein and is believed to be the *Drosophila* equivalent of Pcnt or CG-NAP (5, 9, 10), since Pcnt, CG-NAP, and D-PLP have similar coiled-coil organizations and share a conserved region of 40 aa located in their N-terminal halves. A study using *D-plp*-mutant flies has demonstrated that D-PLP is not essential for mitosis, but rather for the formation of the cilium (9), a cell surface organelle containing a membrane-bound microtubule axoneme at its center. The mutant flies displayed malformed sensory cilia in the mechanosensory and chemosensory neurons, resulting in disturbed neuronal function and a severely uncoordinated phenotype, while mitosis was not dramatically perturbed in *D-plp*-mutant cells. In *Drosophila*, these sensory neurons and sperm are the only ciliated cells. In mammals, ciliated sensory neurons can be found in the olfactory epithelium as olfactory chemosensory neurons that mediate odorant detection, while other somatic cell types are also ciliated. Individual olfactory neurons project a single dendrite to the epithelial surface and an axonal process to the olfactory bulb. Ten to twenty sensory cilia arise from the dendritic knob, a swelling at the apical ending of the dendrite containing multiple basal bodies. These olfactory cilia are embedded in a mucus layer. Diverse odorant receptor proteins, members of the G protein-coupled receptor family, detect odorants at the olfactory epithelium, and type III adenylyl cyclase (ACIII) has been identified as the olfactory epithelium-specific isoform involved in odorant detection (11). Odorant receptors, a heterotrimeric G-protein subunit (Golf), ACIII, a cyclic nucleotide-gated channel, and a Ca^{2+}-activated Cl^- channel

[1] Correspondence: Department of Brain Science, Graduate School of Medicine, Dentistry and Pharmaceutical Sciences, Okayama University, 2-5-1 Shikatacho, Okayama 700-8558, Japan. E-mail: miyoshi@cc.okayama-u.ac.jp

doi: 10.1096/fj.08-124420

are localized at the ciliary membrane of olfactory neurons and are involved in several steps of the chemoelectrical transduction sequence. Odorants dissolve in the mucus and bind to odorant receptors that stimulate Golf, which, in turn, activates ACIII. The subsequent elevation in intralumenal cAMP activates the ion channels, thereby leading to depolarization of membrane voltage and electrical excitation of the neuron. The deletion of each component in the olfactory signaling cascade results in anosmia (12–14). A fine ciliary structure having a high surface-volume ratio is thought to allow efficient signal amplification in the olfactory transduction system. It is well recognized that multiple motile cilia generating fluid flow are present on epithelial cells of the respiratory and the reproductive tract and the ependyma, while most G_0 cells throughout the mammalian body are known to have a nonmotile primary cilium, which singly extends like an antenna into the environment surrounding the cell and possibly transduces sensory stimuli to the cell body.

In our previous study, we analyzed *in vivo* expression of Pcnt in mouse embryos; Pcnt was shown to be localized at the base of primary cilia in embryonic tissues (15). If Pcnt is essential for ciliogenesis in diverse mammalian cell types, Pcnt dysfunction might result in widespread disruption of cilium-mediated events. Inhibited ciliogenesis by down-regulation of Pcnt expression using RNA interference has been shown in cultured mammalian cells (16), while the *in vivo* function of Pcnt remains to be determined. Recently, homozygous truncating mutations in human *PCNT* were shown to cause two types of microcephalic primordial dwarfism (17, 18). It is noteworthy that PCNT is likely to be dispensable for most aspects of human development (17), while the absence of the functional PCNT protein causes short stature and reduced brain size. In this study, we have established and analyzed mice harboring a hypomorphic mutation in the *Pcnt* gene to investigate the implication of Pcnt in ciliogenesis of olfactory chemosensory neurons and other cell types in mammals.

MATERIALS AND METHODS

Animals

Random insertional mutagenesis in mouse embryonic stem cells with a gene trap vector, pU-17, employing the Cre-mutated lox system was carried out at TransGenic, Inc. (Kobe, Japan) (19–21). Clones of a mixed CBA/JN Crj and C57BL/6J genetic background carrying a single copy of the trap vector were selected by analysis of the integration patterns on Southern blots (19). The genomic loci of the vector insertion were determined by 5′-RACE analysis, and one clone with genomic integration of the vector into the *Pcnt* gene was identified. Germline-transmitting chimeras were generated and crossed to wild-type C57BL/6J females to establish a mutant mouse line. The resultant F1-heterozygous mice were backcrossed to the C57BL/6J-strain mice for 8 generations. Experiments were performed in compliance with the Guidelines for Animal Experiments of Okayama University Advanced Science Research Center.

Determination of the vector insertion site and genotyping

Genomic DNA was extracted from mouse tail tips using Wizard SV Genomic DNA Purification System (Promega, Madison, WI, USA) according to the manufacturer's instructions. The precise genomic insertion site of the trap vector was determined by genomic PCR using Ex *Taq* Hot Start Version (Takara, Kyoto, Japan) and the following primers: P1, ctgctcgtcttccatctccacctgggct and P2, ccatacagtcctcttcacatccatgctg (**Fig. 1*B***). PCR included an initial denaturation at 95°C for 3 min, followed by 30 cycles of denaturation at 95°C for 30 s, annealing at 68°C for 30 s, elongation at 72°C for 1 min, and final elongation at 72°C for 5 min. The reaction mixture

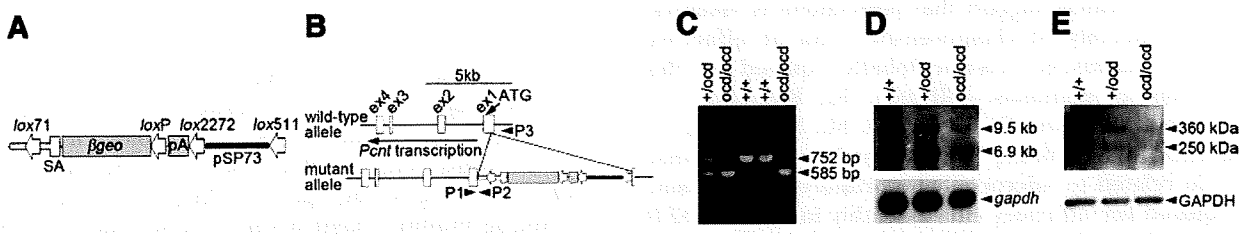

Figure 1. Structure of the *Pcnt*^{ocd} allele and its effects on transcript and protein production. *A*) Structure of the trap vector pU-17. pU-17 is a 9074-bp vector containing 1.8 kb of an intron and a splice acceptor (SA) sequence from the mouse *Engrailed 2* gene, the β-*galactosidase/neomycin-resistance fusion* (β-*geo*) gene, and a polyadenylation signal (pA). A *lox*71 site is located within the intron sequence, and *lox*P, *lox*2272, and *lox*511 sites are located in the downstream of the β-*geo*, pA, and pSP73 vector sequences, respectively. *B*) Integration pattern of the trap vector. Open boxes represent the first 4 exons (ex1–4) of the *Pcnt* gene. ATG start codon and direction of *Pcnt* transcription are indicated. Vector sequence was inserted into the 5′ untranslated region of the first exon (226 bp upstream from the start codon), but in reverse orientation of *Pcnt*. Arrowheads labeled P1–3 represent primers used in PCR-based genotyping. *C*) Representative PCR analysis for genotyping. Three primers (P1–3 in *B*) were used in the same reaction. Wild (+/+), heterozygous (+/ocd), and homozygous (ocd/ocd) genotypes and their corresponding PCR products are shown. DNA fragments of 752 bp from the wild-type allele and 585 bp from the inserted allele were amplified by primer sets P1/P3 and P1/P2, respectively. *D*) Northern blot containing poly(A)+ RNAs from whole neonates at postnatal day 1 from each genotype was hybridized with a riboprobe for *Pcnt* (top). Blot was stripped and then hybridized with a riboprobe for *Gapdh* as a loading control (bottom). Positions of the two *Pcnt* transcripts of 9.5 and 6.9 kb and the *Gapdh* transcript are indicated. *E*) Western blot of whole-cell lysates of embryonic fibroblasts prepared from fetuses carrying each genotype was probed with antibodies to Pcnt (top) or GAPDH as a loading control (bottom). Positions of the two Pcnt isoforms with masses of 360 and 250 kDa and the GAPDH protein are indicated.

was then subjected to agarose gel electrophoresis with visualization of DNA by ethidium bromide staining. The DNA fragment was purified using the Geneclean kit (Bio101, La Jolla, CA, USA), subcloned into the pGEM-T vector (Promega) and sequenced. PCR was also performed for genotyping of mice with the same protocol using primers P1 and P3, (cgactctgtacattgaagcgtgtgcgtg) to detect the wild-type allele and primers P1 and P2 to detect the inserted allele (Fig. 1*B*). The primer sets P1/P3 and P1/P2 gave 752-bp and 585-bp DNA fragments in reaction, respectively (Fig. 1*C*).

Northern blot analysis

cDNA fragments of mouse *Pcnt* (NM_008787, 3838–4629 nt) and of the entire open reading frame of *Gapdh* encoding glyceraldehyde-3-phosphate dehydrogenase (GAPDH) were subcloned into the pBluescript SK(+) vector (Stratagene, La Jolla, CA, USA). Digoxigenin-labeled antisense riboprobes were generated by *in vitro* transcription using the cDNA fragments as templates in the presence of digoxigenin-labeled dUTP (Roche Diagnostics, Basel, Switzerland). Northern blot analysis was performed according to the DIG Application Manual for Filter Hybridization (Roche Diagnostics). Briefly, on postnatal day 1, whole neonates from each genotype were homogenized in TRIzol Reagent (Invitrogen, Carlsbad, CA, USA) with a Polytron homogenizer (Kinematica, Luzern, Switzerland). Total RNA was then isolated using RNeasy Lipid Tissue Midi Kit (Qiagen, Valencia, CA, USA), and poly(A)+ RNA was purified using an mRNA Purification Kit (GE Healthcare, Piscataway, NJ, USA). Eighty nanograms per well of poly(A)+ RNA from each sample was loaded and separated by electrophoresis on a 1% agarose MOPS/formaldehyde gel. Separated RNA was transferred to a Hybond-N+ nylon membrane (GE Healthcare) by capillary transfer and fixed to the membrane by baking at 80°C for 2 h. The membrane was then prehybridized in DIG Easy Hyb (Roche Diagnostics) at 68°C for 30 min and hybridized in the same buffer with the digoxigenin-labeled *Pcnt* riboprobe (100 ng/ml) at 68°C for 16 h. After rinsing in 0.1% SDS and 2× SSC for 10 min at room temperature and in 0.1% SDS and 0.1× SSC for 30 min at 68°C, the membrane was incubated with alkaline phosphatase-conjugated anti-digoxigenin antibody (Roche Diagnostics) at a dilution of 1:10,000 for 30 min at room temperature. The result was visualized by chemiluminescence using CDP-Star (Roche Diagnostics). The membrane was stripped in 50% formamide, 5% SDS, and 50 mM Tris-HCl (pH 7.5) at 80°C for 60 min twice and rehybridized with the *Gapdh* riboprobe.

Preparation of embryonic fibroblasts

Embryonic fibroblasts were prepared from individual embryos bearing each genotype at embryonic day 14.5. The head and internal organs were removed, and the torso was minced and dispersed in 0.25% trypsin for 40 min at 37°C. Embryonic fibroblasts were grown in Dulbecco's modified Eagle's medium (Invitrogen) supplemented with 10% fetal bovine serum, 2 mM glutamine, 100 U/ml penicillin, and 100 μg/ml streptomycin.

Western blot analysis

Embryonic fibroblasts from each genotype were lysed in TNE buffer (150 mM NaCl, 1 mM EDTA, and 20 mM Tris-HCl, pH 7.5) containing 1% Nonidet P-40 in the presence of protease inhibitors and incubated for 1 h over ice. The whole-cell lysates were centrifuged at 16,000 *g* for 20 min, and the resulting supernatants were collected. Prepared lysate samples containing 30 μg of total protein were boiled with SDS sample buffer for 5 min, subjected to SDS-PAGE, and transferred to a PVDF membrane. After blocking with 5% membrane blocking agent (GE Healthcare), the membrane was incubated with a mouse monoclonal antibody to Pcnt (611814; BD Transduction Laboratories, Lexington, KY, USA) at a dilution of 1:500 or to GAPDH (sc-32233, Santa Cruz Biotechnology, Santa Cruz, CA, USA) at a dilution of 1:1,000 for 2 h at room temperature. The membrane was then incubated with HRP-conjugated anti-mouse IgG antibody (Chemicon, Temecula, CA, USA) at a dilution of 1:5000 for 1 h at room temperature. The result was visualized by chemiluminescence using the ECL kit (GE Healthcare).

Immunofluorescence

Six-week-old mice from each genotype were perfusion-fixed with 4% paraformaldehyde in 20 mM PBS. Nasal cavities were decalcified by incubation in 10% EDTA (pH 7.4) for 11 d at room temperature. Postnatal day 1 pups from each genotype were immersion-fixed in 4% paraformaldehyde in 20 mM PBS. The samples were then dehydrated through a graded series of ethanol, cleared in xylene, and embedded in paraffin. Sections were cut at a thickness of 3 μm, mounted onto slides and subjected to immunofluorescence. Deparaffinized sections were postfixed in ice-cold methanol for 10 min, heated in citrate buffer, and permeabilized with 0.3% Triton-X100 in 20 mM PBS. After blocking with Image-iT FX Signal Enhancer (Invitrogen), the sections were incubated with the following primary antibodies for 1 h at room temperature: mouse monoclonal anti-acetylated tubulin (T6793; Sigma, St. Louis, MO, USA; 1:1,000), mouse monoclonal anti-Pcnt (1:200), rabbit polyclonal anti-Pcnt (PRB-432C, 1:500; Covance, Richmond, CA, USA), rabbit polyclonal anti-ACIII (sc-588; 1:100; Santa Cruz Biotechnology) and goat polyclonal anti-IFT88 (EB07088; 1:100; Everest Biotech, Upper Heyford, UK). After being washed with 20 mM PBS, the sections were incubated with the following secondary antibodies for 1 h at room temperature: Alexa Fluor 488- or 594-conjugated goat anti-mouse IgG, Alexa Fluor 488- or 594-conjugated goat anti-rabbit IgG, Alexa Fluor 488-conjugated donkey anti-mouse IgG, and Alexa Fluor 594-conjugated donkey anti-goat IgG (1:500; Invitrogen). The primary and secondary antibodies were diluted in 0.1 M PBS containing 0.3% Triton-X100 and 3% BSA. Finally, the sections were stained with 10 μg/ml Hoechst 33342 (Invitrogen) for 2 min to visualize DNA.

Transmission electron microscopy

We dissected 2.5% glutaraldehyde/2% paraformaldehyde-fixed olfactory mucosae under a stereomicroscope. After being incubated with 1% osmium tetroxide, the mucosae were dehydrated in a graded series of ethanol solutions and embedded. Ultrathin (70–90 nm) sections were prepared using an ultramicrotome, stained with uranyl acetate and lead citrate, and then examined with an electron microscope (H-7100; Hitachi High-Technologies, Tokyo, Japan) operating at 75 kV.

Olfactory performance test

Single-housed 6-wk-old $Pcnt^{ocd/ocd}$ mice and wild-type littermates were food deprived for 18 h. After a piece of corn chip (0.1 g; Tohato, Tokyo, Japan) was buried in the home cage (3 cm under the bedding), the mouse was allowed to search for the food. The time needed to localize the food was measured.

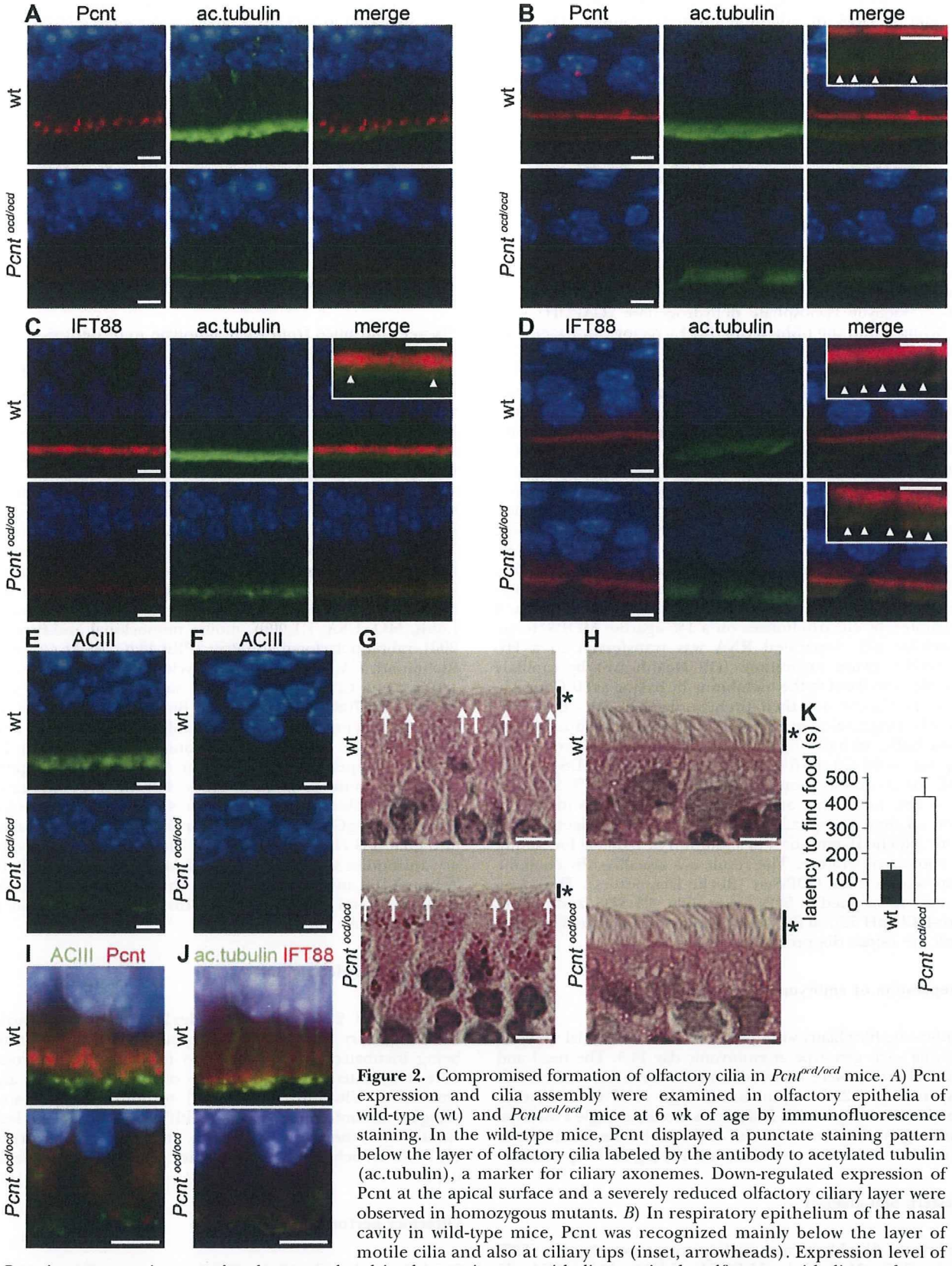

Figure 2. Compromised formation of olfactory cilia in *Pcnt*$^{ocd/ocd}$ mice. *A*) Pcnt expression and cilia assembly were examined in olfactory epithelia of wild-type (wt) and *Pcnt*$^{ocd/ocd}$ mice at 6 wk of age by immunofluorescence staining. In the wild-type mice, Pcnt displayed a punctate staining pattern below the layer of olfactory cilia labeled by the antibody to acetylated tubulin (ac.tubulin), a marker for ciliary axonemes. Down-regulated expression of Pcnt at the apical surface and a severely reduced olfactory ciliary layer were observed in homozygous mutants. *B*) In respiratory epithelium of the nasal cavity in wild-type mice, Pcnt was recognized mainly below the layer of motile cilia and also at ciliary tips (inset, arrowheads). Expression level of Pcnt in mutant mice was also down-regulated in the respiratory epithelium as in the olfactory epithelium, whereas motile cilia formation was not compromised in *Pcnt* mutants, in contrast to decreased assembly of olfactory cilia in mutant olfactory epithelium. *C*) In wild-type olfactory epithelium, the IFT88 subunit of the IFT particle was detected mainly at the apical surface, below the ciliary layer labeled by the acetylated tubulin antibody. In mutants, much of the IFT88

(*continued on next page*)

The test was terminated after the successful localization of the food or after 10 min of unsuccessful searching.

RESULTS

Inhibitory effects of the mutated *Pcnt* allele on transcript and protein production

In the process of random insertional mutagenesis in mouse embryonic stem cells (19–21), one clone with genomic integration of a trap vector into *Pcnt* was identified, and the mutated *Pcnt* allele, provisionally named $Pcnt^{GT(Ayu17ocd)1177Tgjp}$ ($Pcnt^{ocd}$: olfactory cilia defective), was introduced into a C57BL/6J background by multiple-generation backcrossing. The trap vector was revealed to be inserted into the 5′ untranslated region of the first exon of the *Pcnt* gene, but with a reverse orientation of *Pcnt* (Fig. 1*A*, *B*). Polyadenylation trapping by the vector was then thought to be unable to disrupt the *Pcnt* expression, whereas an unknown overlapping gene with an opposite transcriptional orientation might be trapped.

We then explored the possibility that integration of the antisense vector sequence over 9 kb would cause a reduced expression level of *Pcnt* by interfering with *Pcnt* transcription in the mutant mouse tissues. Two *Pcnt* transcripts of 9.5 and 6.9 kb were recognized on the wild-type neonate Northern blot (Fig. 1*D*). The 9.5-kb message encoding the full-length protein of 360 kDa was diminished in the heterozygous mutant and scarcely detectable in the homozygous mutant (Fig. 1*D*). The smaller 6.9-kb transcript that is abundantly expressed in the heart and the skeletal muscle but is scarce in other tissues (22, 23) displayed a lower expression level in the homozygous mutant than in the wild-type or heterozygous mice (Fig. 1*D*).

Western blot analysis was then performed to examine the expression level of the Pcnt protein in whole cell lysates of the embryonic fibroblasts prepared from the fetuses carrying each genotype. The embryonic fibroblasts derived from the homozygous mutant showed very faint Pcnt expression, and the embryonic fibroblasts from the heterozygous embryo had a lower level of expression than the wild-type cells (Fig. 1*E*). Note that the 250-kDa isoform is thought to be derived from the processing of the 360-kDa protein (23). These results indicated that down-regulated expression of the Pcnt protein was achieved by the reverse-oriented vector insertion in the *Pcnt* locus.

The offspring from crosses between mice that were F8-heterozygous for the insertional mutation were genotyped using a PCR-based method (Fig. 1*C*). Wild-type, heterozygous ($Pcnt^{+/ocd}$), and homozygous ($Pcnt^{ocd/ocd}$) pups were born at the expected 1:2:1 Mendelian frequency (39 wild-type, 82 $Pcnt^{+/ocd}$ and 36 $Pcnt^{ocd/ocd}$ of 157 animals analyzed). $Pcnt^{ocd/ocd}$ mice displayed primordial short stature and microcephalus (report in preparation), common features of the two types of the microcephalic primordial dwarfism caused by biallelic loss-of-function mutations in human *PCNT* (17, 18).

Defective assembly of olfactory cilia in $Pcnt^{ocd/ocd}$ mice

Pcnt has been believed to be the mammalian equivalent of D-PLP of *Drosophila* (5, 9, 10), and *D-plp*-mutant flies have been shown to display malformed sensory cilia in the mechanosensory and chemosensory neurons (9). Ciliated chemosensory neurons are also present in mammals as olfactory neurons, which are the specialized neuron type for odorant detection. Thus, we first investigated the formation of olfactory cilia of olfactory neurons in the *Pcnt*-mutant mice.

Sagittal sections of the nasal cavity from 6-wk-old wild-type and $Pcnt^{ocd/ocd}$ mice were investigated by immunofluorescence study. Olfactory (**Fig. 2*A***) and adjacent respiratory (Fig. 2*B*) epithelia were double-stained for Pcnt and acetylated tubulin, a marker for the ciliary axoneme. Pcnt staining yielded a punctate pattern consistent with the distribution of basal bodies in the dendritic knob below the ciliary layer in the wild type (Fig. 2*A*). The down-regulated expression of the Pcnt protein at the apical surface in homozygous mice (Fig. 2*A*) revealed the hypomorphic effect of the $Pcnt^{ocd}$ allele in the olfactory epithelium. Acetylated tubulin

protein was removed from the apical surface of the olfactory epithelium carrying reduced olfactory cilia. *D*) In the respiratory epithelium, staining for the motile ciliary layer and IFT88 was comparable between wild-type and mutant mice. Arrowheads (*C*, *D*; insets) indicate ciliary localization of IFT88. *E*) Immunostaining for ACIII, a ciliary membrane protein required for signal amplification, labeled the olfactory ciliary layer in wild-type olfactory epithelium. Assembly of olfactory cilia positive for ACIII was markedly compromised in mutants. *F*) Antibody to ACIII failed to label cilia in the respiratory epithelium, in agreement with the lack of a signal amplification system in the motile cilia. *G*) Hematoxylin-and-eosin (H&E) staining of olfactory epithelia from 6-wk-old wild-type and $Pcnt^{ocd/ocd}$ mice revealed decreased thickness of the cilia layer (asterisks) in mutants. Dendritic knobs (arrows) were observed at the apical surface in both wild-type and mutant mice. *H*) In respiratory epithelia stained with H&E, cilia layer (asterisks) was comparable between wild-type and mutant mice. *I*) In the superior part of the nasal cavity of the wild-type pup at postnatal day 1, olfactory cilia assembly was demonstrated by expression of ACIII (green) close to punctate staining of Pcnt (red) at the apical surface. In homozygous mutant pups, immunoreactivity for ACIII and Pcnt was rarely observed in the nasal cavity. *J*) Olfactory epithelium of wild-type neonates displayed developing cilia labeled by the antibody to acetylated tubulin (green) and contiguous localization of IFT88 (red) at the apical surface. Both olfactory cilia assembly and IFT88 localization were diminished in *Pcnt*-mutant pups. Nuclei were labeled with Hoechst (blue) (*A-F*, *I*, *J*). Scale bars = 5 μm. *K*) Six-week-old $Pcnt^{ocd/ocd}$ mice (white bar; n=13) revealed a significantly increased mean latency in finding a hidden food morsel compared with wild-type littermates (black bar; n=14) in the olfactory performance test; $P < 0.01$, Student's t test. Data are means ± SE.

staining demonstrated that the formation of olfactory cilia was markedly compromised in the mutant olfactory epithelium (Fig. 2*A*). The respiratory epithelium of the nasal cavity bears multiple motile cilia that transport mucus to remove ingested bacteria and dust. The Pcnt protein was recognized mainly at the base of these motile cilia and also at the ciliary tips in wild-type mice (Fig. 2*B*). The expression level of Pcnt in the homozygous mutants was down-regulated in the respiratory epithelium (Fig. 2*B*), as well as in the olfactory epithelium. Formation of motile cilia in the respiratory epithelium was, however, not compromised by the hypomorphic mutation of *Pcnt* (Fig. 2*B*), in contrast to the decreased assembly of olfactory cilia in the mutant olfactory epithelium. Intraflagellar transport (IFT) is a highly conserved system and essential for the assembly and maintenance of flagella and motile and nonmotile cilia (24, 25). IFT particles, protein complexes composed of several different subunits, transport cargo along microtubules by motor proteins, such as kinesin and dynein, between the cell body and the tip of the cilium/flagellum. Localization of the IFT88 subunit of the IFT particle was then investigated in the olfactory (Fig. 2*C*) and respiratory (Fig. 2*D*) epithelium. In the wild-type mice, IFT88 was detected mainly at the apical surface of the olfactory (Fig. 2*C*) and respiratory (Fig. 2*D*) epithelium below the ciliary layer labeled by the antibody to acetylated tubulin. In addition, a fraction of the IFT88 subunit was localized within the ciliary layer of the wild-type epithelia (Fig. 2*C, D*). In the mutant mice, much of the IFT88 protein was removed from the apical surface of the olfactory epithelium (Fig. 2*C*), while IFT88 localization in the respiratory epithelium was not affected by the hypomorphic mutation of *Pcnt* (Fig. 2*D*). The antibody to ACIII also labeled the ciliary layer in the wild-type olfactory epithelium, while ACIII-positive olfactory cilia were markedly decreased in the mutant (Fig. 2*E*). In the respiratory epithelium, motile cilia were undetectable by the ACIII antibody (Fig. 2*F*), in agreement with the lack of the signal amplification system required for odorant detection. Structural defects of the olfactory cilia layer and proper formation of respiratory cilia in the mutant mice were confirmed by hematoxylin-and-eosin staining of the nasal cavity sections (Fig. 2*G, H*). Ultrastructural observation by transmission electron microscopy showed the thinned ciliary layer with impaired development of the distal segments of the olfactory cilia in the mutant olfactory epithelium (Supplemental Fig. 1).

Sagittal sections of the nasal cavity from postnatal day 1 newborn pups were next double-stained for ACIII and Pcnt (Fig. 2*I*). In the wild-type neonates, assembly of olfactory cilia was demonstrated by the expression of ACIII close to the punctate staining of Pcnt at the apical surface. In contrast, immunoreactivity for ACIII and Pcnt was rarely observed in the homozygous mutant pups. Improperly formed cilia labeled by the antibody to acetylated tubulin and decreased localization of IFT88 at the apical surface were also observed in the olfactory epithelium of the mutant pups (Fig. 2*J*). These observations indicate that the defective ciliogenesis is apparent from birth in the mutant mice.

To test whether the *Pcnt*-mutant mice had impaired olfaction, an olfactory performance test was carried out at 6 wk of age. $Pcnt^{ocd/ocd}$ mice took approximately 3 times as much time to locate a hidden food morsel as their wild-type littermates (Fig. 2*K*), in accordance with the defective assembly of olfactory cilia.

Unaffected assembly of cilia and flagella in body regions other than the olfactory epithelium in $Pcnt^{ocd/ocd}$ mice

It is established that dysfunction of motile cilia of the ependymal cells and the bronchiolar epithelial cells, as well as primary cilia of the renal tubular epithelial cells, is linked to the pathogenesis of human disorders, such as hydrocephalus, respiratory tract infections, and polycystic kidney disease (25). Ciliary assembly of the ependymal cells (**Fig. 3*A***) and the bronchiolar (Fig. 3*B*) and renal tubular (Fig. 3*C*) epithelial cells was not affected by the hypomorphic mutation of *Pcnt*. Anomalies of sperm flagella, which share the "9 + 2" microtubule architecture with motile cilia, are known to cause male infertility (25). In the *Pcnt*-mutant male mice, proper assembly of sperm flagella was observed in the epididymis (Fig. 3*D*). These results are in accordance with our observation that none of the *Pcnt*-mutant mice tested in the study suffered from hydrocephalus or renal cysts, even in the late stage of life, and that the mutant male mice were fertile (unpublished data). Dysfunction of specialized nonmotile cilia that connect the inner and outer segments of photoreceptor cells has been suggested to underlie human retinal degenerative diseases (25). The retina of $Pcnt^{ocd/ocd}$ mice appeared to be intact, with normal outer nuclear and photoreceptor layers (Fig. 3*E*).

DISCUSSION

Our results have shown that integration of a trap vector into the first exon in the reverse direction produced a hypomorphic allele of the *Pcnt* gene. Low-level residual Pcnt immunoreactivity in the homozygous mutants (Figs. 1*E* and 2*A, B, I*) seems to reflect incomplete disruption of *Pcnt* gene expression by the vector insertion. The mutation decreased expression levels of 9.5- and 6.9-kb *Pcnt* transcripts, with a preferential effect on the former (Fig. 1*D*), most likely because the 6.9-kb transcript arose from the utilization of an alternative transcription initiation site located ~20 kb downstream of the vector integration site (23). Homozygous insertion of the vector sequence into the 5′ untranslated region did not completely inhibit transcription of the 9.5-kb message (Fig. 1*B, D*). The residual expression of the 9.5-kb transcript in the homozygous mutant (Fig. 1*D*) might be obtained due to a downstream shift in transcription initiation. Multitissue analysis has re-

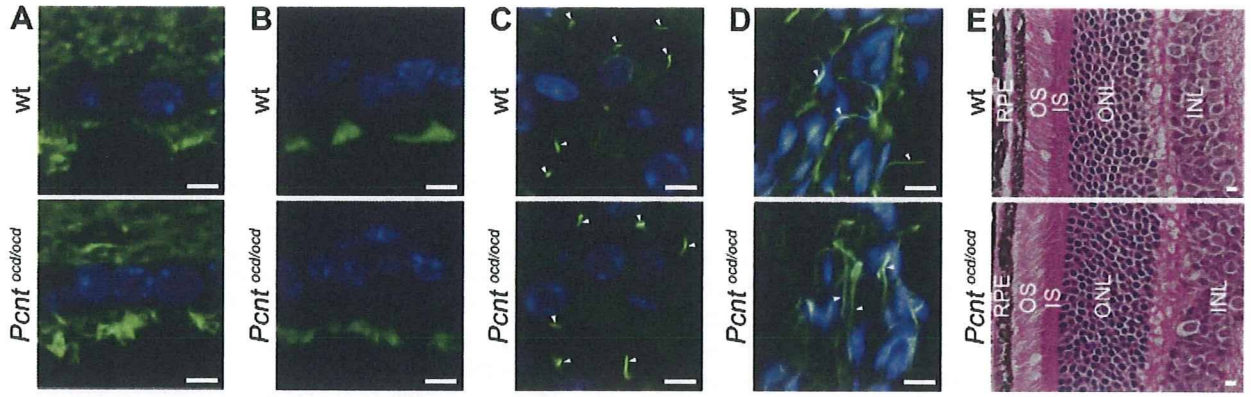

Figure 3. Unaffected assembly of cilia and flagella in cell types other than olfactory neurons in $Pcnt^{ocd/ocd}$ mice. *A–C*) Sections of ependyma of lateral ventricle (*A*), bronchiole (*B*), and renal tubule (*C*) from wild-type (wt) and $Pcnt^{ocd/ocd}$ mice at 6 wk of age were immunostained with antibodies to acetylated tubulin. Mutant mice displayed normal assembly of ependymal and bronchiolar motile cilia and of renal primary cilia. *D*) Sperm flagella in the epididymis were stained with antibodies to acetylated tubulin. Flagellar formation was comparable between wild-type and mutant mice. Arrowheads indicate cilia and flagella (*C, D*). Nuclei were labeled with Hoechst (blue). *E*) H&E staining of retinal sections from wild-type and $Pcnt^{ocd/ocd}$ mice revealed intact photoreceptor cells in the mutants. RPE, retinal pigment epithelium; OS, outer segment; IS, inner segment; ONL, outer nuclear layer; INL, inner nuclear layer. Scale bars = 5 μm.

vealed expression of the 6.9-kb message to be largely confined to heart and skeletal muscle in mice (22, 23).

Polyadenylation trapping by the vector might disrupt the expression of an unknown overlapping gene with a reverse transcriptional orientation of *Pcnt*. No reverse-oriented genes have been annotated on the genomic contigs in the 5′ region of *Pcnt* (data not shown), while a noncoding RNA gene may exist in the region (21). We therefore cannot exclude the possibility that abnormalities observed in $Pcnt^{ocd/ocd}$ mice reflect the altered expression of the overlapping gene. It has been reported that integration of the trap vector into the promoter region in reverse orientation generated a hypomorphic allele of the *Kpnb1* gene (26).

Hypomorphic mutation of *Pcnt* resulted in disturbed cilia assembly of olfactory chemosensory neurons (Fig. 2). Diminished IFT88 labeling in the mutant olfactory epithelium (Fig. 2*C, J*) can be considered as a consequence of impaired development of olfactory cilia. The adult mutant mice displayed reduced olfactory performance but were still able to locate a hidden food pellet (Fig. 2*K*). Insufficiency of olfactory cilia was apparent from birth (Fig. 2*I, J*), while mutant pups showed nipple-search behavior and were raised to weaning (unpublished data). These observations indicate that olfactory performance was not completely compromised by the homozygous mutation and that improperly formed cilia still maintained some olfactory function in the mutants. Assembly of cilia in ependymal cells (Fig. 3*A*) and nasal respiratory (Fig. 2*B, D*), bronchiolar (Fig. 3*B*) and renal tubular (Fig. 3*C*) epithelial cells was comparable between the homozygous mutants and wild-type animals. In addition, the *Pcnt*-mutant mice revealed normal formation of sperm flagella (Fig. 3*D*) and intact photoreceptors (Fig. 3*E*). These results suggest that Pcnt is dispensable or that a decreased level of Pcnt expression is sufficient for ciliogenesis in these cell types. It is noteworthy in this regard that flies with a mutation in the gene encoding D-PLP, the *Drosophila* equivalent of Pcnt, displayed malformed sensory cilia in the chemosensory and mechanosensory neurons (9), suggesting that these PACT domain-containing proteins might play a conserved role, from invertebrates to vertebrates, preferentially in the assembly of specialized sensory cilia at the apical end of sensory neurons.

In contrast to the lack of severe pathological abnormalities in the *Pcnt*-mutants, $Tg737^{orpk}$ mice that harbor a hypomorphic mutation in the gene encoding IFT88 display hydrocephalus, renal cysts, and ductal abnormalities in the pancreas and the liver and normally die within 2 wk of birth (27–31). $Tg737^{orpk}$ mice display stunted primary cilia in renal, biliary, and pancreatic epithelia and underdeveloped ependymal cilia (28–31), showing that general disruption of the IFT machinery results in systemic and lethal abnormalities. Selective structural defects in chemosensory cilia of olfactory neurons have also been found in mice with disruption of causative genes for Bardet-Biedl syndrome (BBS), a pleiotropic genetic disorder characterized by obesity, retinal degeneration, polydactyly, renal and limb malformations, learning disabilities, and hypogenitalism (25). The molecular basis of BBS remains unclear, while BBS proteins encoded by 14 responsible genes (*BBS1–14*) so far identified are located in the basal body and cilia. BBS patients have partial or complete anosmia (32), and *Bbs1*-, *Bbs2*-, *Bbs4*-, and *Bbs6*-null mice reveal impaired olfactory function (32–34). The severe reduction of the ciliated border of the olfactory, but not the respiratory, epithelium was observed in *Bbs1*-, *Bbs4*-, and *Bbs6*-null mice (32, 34). On the other hand, *Bbs1*- and *Bbs4*-null mice displayed normal renal cilia (25, 35). Seven of the most conserved

BBS proteins form a stable complex that binds pericentriolar material 1 (PCM-1) (36), and PCM-1 is associated with Pcnt (4, 37) and plays a critical role in ciliogenesis (36, 38). Many questions remain concerning the mechanisms by which impairment of a particular cilia-related component affects some particular subset of ciliary structural or functional features, while leaving others intact (39).

In humans, biallelic truncating mutations in *PCNT* cause two types of microcephalic primordial dwarfism (17, 18). Dwarf patients with *PCNT* mutation have not been reported to have reduced olfactory performance, though restricted olfaction occurring at birth might not be recognized without olfactory tests. Some genes involved in assembly or function of cilia may have additional functions unrelated to cilia (39), and it remains to be determined whether microcephalus and dwarfism caused by *PCNT* mutation are cilia-related or -unrelated symptoms. Cultured cells from dwarf patients with biallelic mutations in *PCNT* have been shown to display defective ataxia-telangiectasia and Rad3-related (ATR)-dependent DNA damage signaling (17) or disorganized mitotic spindles and missegregation of chromosomes (18), raising the possibility that perturbation of cell division or reduced cell survival results in globally reduced cell number and growth restriction causing primordial dwarfism. As expected, $Pcnt^{ocd/ocd}$ mice replicated primordial short stature and microcephalus (report in preparation). Further analysis of $Pcnt^{ocd/ocd}$ mice may provide insight into cellular pathways responsible for the brain and body size phenotypes. FJ

This work was supported by Grants-in-Aid for Scientific Research (Kakenhi; grant 19591355).

REFERENCES

1. Doxsey, S. J., Stein, P., Evans, L., Calarco, P. D., and Kirschner, M. (1994) Pericentrin, a highly conserved centrosome protein involved in microtubule organization. *Cell* **76,** 639–650
2. Takahashi, M., Shibata, H., Shimakawa, M., Miyamoto, M., Mukai, H., and Ono, Y. (1999) Characterization of a novel giant scaffolding protein, CG-NAP, that anchors multiple signaling enzymes to centrosome and the golgi apparatus. *J. Biol. Chem.* **274,** 17267–17274
3. Flory, M. R., Moser, M. J., Monnat, R.J., Jr., and Davis, T. N. (2000) Identification of a human centrosomal calmodulin-binding protein that shares homology with pericentrin. *Proc. Natl. Acad. Sci. U. S. A.* **97,** 5919–5923
4. Li, Q., Hansen, D., Killilea, A., Joshi, H. C., Palazzo, R. E., and Balczon, R. (2001) Kendrin/pericentrin-B, a centrosome protein with homology to pericentrin that complexes with PCM-1. *J. Cell Sci.* **114,** 797–809
5. Gillingham, A. K., and Munro, S. (2000) The PACT domain, a conserved centrosomal targeting motif in the coiled-coil proteins AKAP450 and pericentrin. *EMBO Rep.* **1,** 524–529
6. Dictenberg, J. B., Zimmerman, W., Sparks, C. A., Young, A., Vidair, C., Zheng, Y., Carrington, W., Fay, F. S., and Doxsey, S. J. (1998) Pericentrin and gamma-tubulin form a protein complex and are organized into a novel lattice at the centrosome. *J. Cell Biol.* **141,** 163–174
7. Takahashi, M., Yamagiwa, A., Nishimura, T., Mukai, H., and Ono, Y. (2002) Centrosomal proteins CG-NAP and kendrin provide microtubule nucleation sites by anchoring γ-tubulin ring complex. *Mol. Biol. Cell* **13,** 3235–3245
8. Zimmerman, W. C., Sillibourne, J., Rosa, J., and Doxsey, S. J. (2004) Mitosis-specific anchoring of γ tubulin complexes by pericentrin controls spindle organization and mitotic entry. *Mol. Biol. Cell* **15,** 3642–3657
9. Martinez-Campos, M., Basto, R., Baker, J., Kernan, M., and Raff, J. W. (2004) The *Drosophila* pericentrin-like protein is essential for cilia/flagella function, but appears to be dispensable for mitosis. *J. Cell Biol.* **165,** 673–683
10. Kawaguchi, S., and Zheng, Y. (2004) Characterization of a *Drosophila* centrosome protein CP309 that shares homology with Kendrin and CG-NAP. *Mol. Biol. Cell* **15,** 37–45
11. Bakalyar, H. A., and Reed, R. R. (1990) Identification of a specialized adenylyl cyclase that may mediate odorant detection. *Science* **250,** 1403–1406
12. Brunet, L. J., Gold, G. H., and Ngai, J. (1996) General anosmia caused by a targeted disruption of the mouse olfactory cyclic nucleotide-gated cation channel. *Neuron* **17,** 681–693
13. Belluscio, L., Gold, G. H., Nemes, A., and Axel, R. (1998) Mice deficient in G(olf) are anosmic. *Neuron* **20,** 69–81
14. Wong, S. T., Trinh, K., Hacker, B., Chan, G. C., Lowe, G., Gaggar, A., Xia, Z., Gold, G. H., and Storm, D. R. (2000) Disruption of the type III adenylyl cyclase gene leads to peripheral and behavioral anosmia in transgenic mice. *Neuron* **27,** 487–497
15. Miyoshi, K., Onishi, K., Asanuma, M., Miyazaki, I., Diaz-Corrales, F. J., and Ogawa, N. (2006) Embryonic expression of pericentrin suggests universal roles in ciliogenesis. *Dev. Genes Evol.* **216,** 537–542
16. Jurczyk, A., Gromley, A., Redick, S., San Agustin, J., Witman, G., Pazour, G. J., Peters, D. J., and Doxsey, S. (2004) Pericentrin forms a complex with intraflagellar transport proteins and polycystin-2 and is required for primary cilia assembly. *J. Cell Biol.* **166,** 637–643
17. Griffith, E., Walker, S., Martin, C. A., Vagnarelli, P., Stiff, T., Vernay, B., Al Sanna, N., Saggar, A., Hamel, B., Earnshaw, W. C., Jeggo, P. A., Jackson, A. P., and O'Driscoll, M. (2008) Mutations in pericentrin cause Seckel syndrome with defective ATR-dependent DNA damage signaling. *Nat. Genet.* **40,** 232–236
18. Rauch, A., Thiel, C. T., Schindler, D., Wick, U., Crow, Y. J., Ekici, A. B., van Essen, A. J., Goecke, T. O., Al-Gazali, L., Chrzanowska, K. H., Zweier, C., Brunner, H. G., Becker, K., Curry, C. J., Dallapiccola, B., Devriendt, K., Dörfler, A., Kinning, E., Megarbane, A., Meinecke, P., Semple, R. K., Spranger, S., Toutain, A., Trembath, R. C., Voss, E., Wilson, L., Hennekam, R., de Zegher, F., Dörr, H. G., and Reis, A. (2008) Mutations in the pericentrin (PCNT) gene cause primordial dwarfism. *Science* **319,** 816–819
19. Araki, K., Imaizumi, T., Sekimoto, T., Yoshinobu, K., Yoshimuta, J., Akizuki, M., Miura, K., Araki, M., and Yamamura, K. (1999) Exchangeable gene trap using the Cre/mutated lox system. *Cell. Mol. Biol. (Noisy-le-grand).* **45,** 737–750
20. Taniwaki, T., Haruna, K., Nakamura, H., Sekimoto, T., Oike, Y., Imaizumi, T., Saito, F., Muta, M., Soejima, Y., Utoh, A., Nakagata, N., Araki, M., Yamamura, K., and Araki, K. (2005) Characterization of an exchangeable gene trap using pU-17 carrying a stop codon-beta geo cassette. *Dev. Growth Differ.* **47,** 163–172
21. Yamamura, K., and Araki, K. (2008) Gene trap mutagenesis in mice: new perspectives and tools in cancer. *Res. Cancer Sci.* **99,** 1–6
22. Flory, M. R., and Davis, T. N. (2003) The centrosomal proteins pericentrin and kendrin are encoded by alternatively spliced products of one gene. *Genomics* **82,** 401–405
23. Miyoshi, K., Asanuma, M., Miyazaki, I., Matsuzaki, S., Tohyama, M., and Ogawa, N. (2006) Characterization of pericentrin isoforms in vivo. *Biochem. Biophys. Res. Commun.* **351,** 745–749
24. Rosenbaum, J. L., and Witman, G. B. (2002) Intraflagellar transport. *Nat. Rev. Mol. Cell. Biol.* **3,** 813–825
25. Pan, J., Wang, Q., and Snell, W. J. (2005) Cilium-generated signaling and cilia-related disorders. *Lab. Invest.* **85,** 452–463
26. Miura, K., Yoshinobu, K., Imaizumi, T., Haruna, K., Miyamoto, Y., Yoneda, Y., Nakagata, N., Araki, M., Miyakawa, T., Yamamura, K., and Araki, K. (2006) Impaired expression of importin/karyopherin beta1 leads to post-implantation lethality. *Biochem. Biophys. Res. Commun.* **341,** 132–138

27. Moyer, J. H., Lee-Tischler, M. J., Kwon, H. Y., Schrick, J. J., Avner, E. D., Sweeney, W. E., Godfrey, V. L., Cacheiro, N. L., Wilkinson, J. E., and Woychik, R. P. (1994) Candidate gene associated with a mutation causing recessive polycystic kidney disease in mice. *Science* **264,** 1329–1333
28. Pazour, G. J., Dickert, B. L., Vucica, Y., Seeley, E. S., Rosenbaum, J. L., Witman, G. B., and Cole, D. G. (2000) Chlamydomonas IFT88 and its mouse homologue, polycystic kidney disease gene tg737, are required for assembly of cilia and flagella. *J. Cell Biol.* **151,** 709–718
29. Taulman, P. D., Haycraft, C. J., Balkovetz, D. F., and Yoder, B. K. (2001) Polaris, a protein involved in left-right axis patterning, localizes to basal bodies and cilia. *Mol. Biol. Cell* **12,** 589–599
30. Cano, D. A., Murcia, N. S., Pazour, G. J., and Hebrok, M. (2004) Orpk mouse model of polycystic kidney disease reveals essential role of primary cilia in pancreatic tissue organization. *Development* **131,** 3457–3467
31. Zhang, Q., Davenport, J. R., Croyle, M. J., Haycraft, C. J., and Yoder, B. K. (2005) Disruption of IFT results in both exocrine and endocrine abnormalities in the pancreas of Tg737(orpk) mutant mice. *Lab. Invest.* **85,** 45–64
32. Kulaga, H. M., Leitch, C. C., Eichers, E. R., Badano, J. L., Lesemann, A., Hoskins, B. E., Lupski, J. R., Beales, P. L., Reed, R. R., and Katsanis, N. (2004) Loss of BBS proteins causes anosmia in humans and defects in olfactory cilia structure and function in the mouse. *Nat. Genet.* **36,** 994–998
33. Nishimura, D. Y., Fath, M., Mullins, R. F., Searby, C., Andrews, M., Davis, R., Andorf, J. L., Mykytyn, K., Swiderski, R. E., Yang, B., Carmi, R., Stone, E. M., and Sheffield, V. C. (2004) Bbs2-null mice have neurosensory deficits, a defect in social dominance, and retinopathy associated with mislocalization of rhodopsin. *Proc. Natl. Acad. Sci. U. S. A.* **101,** 16588–16593
34. Ross, A. J., May-Simera, H., Eichers, E. R., Kai, M., Hill, J., Jagger, D. J., Leitch, C. C., Chapple, J. P., Munro, P. M., Fisher, S., Tan, P. L., Phillips, H. M., Leroux, M. R., Henderson, D. J., Murdoch, J. N., Copp, A. J., Eliot, M. M., Lupski, J. R., Kemp, D. T., Dollfus, H., Tada, M., Katsanis, N., Forge, A., and Beales, P. L. (2005) Disruption of Bardet–Biedl syndrome ciliary proteins perturbs planar cell polarity in vertebrates. *Nat. Genet.* **37,** 1135–1140
35. Mykytyn, K., Mullins, R. F., Andrews, M., Chiang, A. P., Swiderski, R. E., Yang, B., Braun, T., Casavant, T., Stone, E. M., and Sheffield, V. C. (2004) Bardet-Biedl syndrome type 4 (BBS4)-null mice implicate Bbs4 in flagella formation but not global cilia assembly. *Proc. Natl. Acad. Sci. U. S. A.* **101,** 8664–8669
36. Nachury, M. V., Loktev, A. V., Zhang, Q., Westlake, C. J., Perănen, J., Merdes, A., Slusarski, D. C., Scheller, R. H., Bazan, J. F., Sheffield, V. C., and Jackson, P. K. (2007) A core complex of BBS proteins cooperates with the GTPase Rab8 to promote ciliary membrane biogenesis. *Cell* **129,** 1201–1213
37. Kubo, A., and Tsukita, S. (2003) Non-membranous granular organelle consisting of PCM-1: subcellular distribution and cell-cycle-dependent assembly/disassembly. *J. Cell Sci.* **116,** 919–928
38. Kim, J., Krishnaswami, S. R., and Gleeson, J. G. (2008) CEP290 interacts with the centriolar satellite component PCM-1 and is required for Rab8 localization to the primary cilium. *Hum. Mol. Genet.* **17,** 3796–3805
39. Marshall, W. F. (2008) The cell biological basis of ciliary disease. *J. Cell Biol.* **180,** 17–21

Received for publication November 12, 2008.
Accepted for publication May 7, 2009.

Journal of Neurochemistry JNC

JOURNAL OF NEUROCHEMISTRY | 2009 | 110 | 496–508 doi: 10.1111/j.1471-4159.2009.06099.x

Tumor necrosis factor receptor-associated protein 1 regulates cell adhesion and synaptic morphology via modulation of N-cadherin expression

Kyoko Kubota,*,[1] Kiyoshi Inoue,*,†,[1] Ryota Hashimoto,‡,§,¶ Natsuko Kumamoto,* Asako Kosuga,** Masahiko Tatsumi,** Kunitoshi Kamijima,** Hiroshi Kunugi,¶ Nakao Iwata,†† Norio Ozaki,‡‡ Masatoshi Takeda§ and Masaya Tohyama*

*Department of Anatomy and Neuroscience, Osaka University Graduate School of Medicine, Suita, Osaka, Japan

†Center for Behavioral Neuroscience, Yerkes National Primate Research Center, Emory University, Atlanta, Georgia, USA

‡The Osaka-Hamamatsu Joint Research Center for Child Mental Development, Osaka University Graduate School of Medicine, Suita, Osaka, Japan

§Department of Psychiatry, Osaka University Graduate School of Medicine, Suita, Osaka, Japan

¶Department of Mental Disorder Research, National Institute of Neuroscience, National Center of Neurology and Psychiatry, Kodaira, Tokyo, Japan

**Department of Psychiatry, Showa University School of Medicine, Shinagawaku, Tokyo, Japan

††Department of Psychiatry, Fujita Health University School of Medicine, Toyoake, Aichi, Japan

‡‡Department of Psychiatry, Nagoya University Graduate School of Medicine, Nagoya, Aichi, Japan

Abstract

An increase in serum tumor necrosis factor-α (TNF-α) levels is closely related to the pathogenesis of major depression. However, the underlying molecular mechanism between this increase and impairment of brain function remains elusive. To better understand TNF-α/TNF receptor 1 signaling in the brain, we analyzed the brain distribution and function of tumor necrosis factor receptor-associated protein 1 (TRAP1). Here we show that TRAP1 is broadly expressed in neurons in the mouse brain, including regions that are implicated in the pathogenesis of major depression. We demonstrate that small interfering RNA-mediated knockdown of TRAP1 in a neuronal cell line decreases tyrosine phosphorylation of STAT3, followed by a reduction of the transcription factor E2F1, resulting in a down-regulation of N-cadherin, and affects the adhesive properties of the cells. In addition, in cultured hippocampal neurons, reduced expression of N-cadherin by TRAP1 knockdown influences the morphology of dendritic spines. We also report a significant association between several single nucleotide polymorphisms in the *TRAP1* gene and major depression. Our findings indicate that TRAP1 mediates TNF-α/TNF receptor 1 signaling to modulate N-cadherin expression and to regulate cell adhesion and synaptic morphology, which may contribute to the pathogenesis of major depression.

Keywords: cell adhesion, N-cadherin, small interfering RNA, synaptic morphology, tumor necrosis factor receptor, tumor necrosis factor receptor-associated protein 1.

J. Neurochem. (2009) **110**, 496–508.

Received/accepted April 2, 2009.

Address correspondence and reprint requests to Kiyoshi Inoue, Center for Behavioral Neuroscience, Yerkes National Primate Research Center, Emory University School of Medicine, 954 Gatewood Road NE, Atlanta, GA 30322, USA. E-mail: kinoue@emory.edu

[1]These authors contributed equally to this study.

Abbreviations used: DiI, 1,1′-dioctadecyl-3,3,3′,3′-tetramethylindocarbocyanine perchlorate; HSP90, heat shock protein 90; PBS, phosphate buffered saline; siRNA, small interfering RNA; siTRAP1, siRNAs against TRAP1; SNP, single nucleotide polymorphism; STAT, Signal Transducers and Activator of Transcription; TBS, Tris-bufferd saline; TNF, tumor necrosis factor; TNFR, tumor necrosis factor receptor; TRAP1, tumor necrosis factor receptor-associated protein 1.

Tumor necrosis factor-α (TNF-α), which initiates inflammatory immune responses, has been implicated in the pathogenesis of major depression by several lines of evidence (Lanquillon *et al.* 2000; Reichenberg *et al.* 2001; Hestad *et al.* 2003; Jun *et al.* 2003; Tuglu *et al.* 2003; Simen *et al.* 2006; Irwin and Miller 2007). For example, a number of studies have reported that the plasma level of TNF-α is elevated in patients with major depression and can be corrected by anti-depressants in therapy-responders (Lanquillon *et al.* 2000; Hestad *et al.* 2003; Tuglu *et al.* 2003). Infectious and autoimmune diseases are also known to up-regulate serum TNF-α and results in depressive symptoms (Reichenberg *et al.* 2001; Irwin and Miller 2007). Moreover, polymorphisms in the *TNF-α* gene confer susceptibility to major depression (Jun *et al.* 2003). However, little is known about how TNF-α influences neuronal function in the brain.

Tumor necrosis factor-α is a multifunctional cytokine that plays key roles in inflammation, immune response, cell differentiation, proliferation and apoptosis (Pan *et al.* 1997; Baud and Karin 2001). TNF-α is thought to exert its physiological activity through binding to two distinct receptors: type I tumor necrosis factor receptor (TNFR1) and type II tumor necrosis factor receptor (TNFR2). The TNF-α/TNFR1 signaling system has been well documented; it activates several signal transduction pathways including c-*Jun* N-terminal kinase, nuclear factor-κB and caspases (Wallach *et al.* 1999; Baud and Karin 2001; Karin and Lin 2002).

Tumor necrosis factor receptor-associated protein 1 (TRAP1) was initially identified as an interacting protein that binds the intracellular domain of TNFR1 *in vitro* (Song *et al.* 1995). However, the role of TRAP1 in signal transduction through TNFR1 is unknown. TRAP1 is a member of the heat shock protein 90 (HSP90) family and possesses ATPase activity, but lacks chaperone activity (Felts *et al.* 2000). TRAP1 has also been reported to interact with the retinoblastoma protein and tumor suppressors EXT1 and EXT2, but the functional implications of these interactions are unsolved (Chen *et al.* 1996; Simmons *et al.* 1999).

Here we report that TRAP1 works synergistically with TNFR1 to modulate the expression of the cell adhesion molecule N-cadherin, and alters inter-cellular adhesion of neuronal cells. Furthermore, we demonstrate that TRAP1 regulates the morphology of dendritic spines in cultured hippocampal neurons. In addition, we found four single nucleotide polymorphisms (SNPs) changes in the *TRAP1* gene which may predispose patients to major depression.

Materials and methods

In situ hybridization

In situ hybridization was performed as described previously with minor modifications (Furukawa *et al.* 1997). Details are available in the Appendix S1.

Cell culture

Cell cultures were performed as previously described (Kubota *et al.* 2009). Primary hippocampal cultures were prepared from E18 Wistar rat embryos.

Preparation of siRNAs and transfection

Small interfering RNAs (siRNAs) specific to human TRAP1 (si*GENOME SMART* pool siRNA, M-010104-00, GE Healthcare, Buckinghamshire, England), human TNFRSF1A (M-005197-00, GE Healthcare), human TNFRSF1B (M-003934-00, Thermo Fisher Scientific, Waltham, MA, USA) and rat TRAP1 (Accell siRNA, A-08280409, Thermo Fisher Scientific) were purchased. The non-targeting siRNAs for the human genome (si*CONTROL* Non-Targeting siRNA #1, GE Healthcare) or the rat genome (Accell Non-targeting siRNA #1, Thermo Fisher Scientific) were used as a control. siRNA transfection was performed with Lipofectamine RNAiMAX (Invitrogen, Carlsbad, CA, USA) according to the manufacturer's protocol. SH-SY5Y cells were grown to 20–30% confluence in a 3.5 cm dish, transfected with 25 nM or 50 nM siRNA against TRAP1, 50 nM siRNA against TNFR1, TNFR2, or control siRNA, and then incubated for 24, 48 and 72 h. Cultured hippocampal neurons were transfected with 100 nM siRNA specific for TRAP1 mRNA at day 17 *in vitro* (DIV17) and then incubated for 72 h.

Western blot analysis and Immunocytochemistry

Western blot analysis and Immunocytochemistry were done as described (Kubota *et al.* 2009). Antibodies used are listed in the Appendix S1. Cells were fixed with cold methanol for 20 min at −20°C or with 2.5% paraformaldehyde/phosphate buffered saline (PBS) for 20 min for staining of TRAP1 or N-cadherin, respectively. All experiments were performed at least three times.

Cell aggregation assay

The cell aggregation assay was performed as previously described (Takeichi and Nakagawa 2001) with minor modifications. Monolayer cultures of SH-SY5Y cells were prepared by incubating them for 72 h after siRNA transfection. Single cells were harvested in HEPES-buffered Ca^{2+}-, Mg^{2+}-free salt solution (10 mM HEPES-NaOH in Ca^{2+}-and Mg^{2+}-free saline, pH 7.4) containing 0.01% trypsin and 10 mM $CaCl_2$ for 30 min at 37°C. The cells were centrifuged for 3 min at 800 *g* and suspended at 5×10^4 cells/ml in HEPES-buffered Ca^{2+}-, Mg^{2+}-free salt solution containing 1 mM $CaCl_2$. Five hundred μl of cells were added to each well of a bovine serum albumin-coated 24 well tissue culture plate. EGTA was added at 1 mM where indicated. Then the plate was shaken on a gyrating shaker (4630JPN, Barnstead International, Dubuque, IA, USA) for 30 min at 37°C. The aggregation process was examined using a fluorescence microscope (IX71, Olympus, Tokyo, Japan).

Real-time RT-PCR

Forty-eight hours after transfection, total RNA was extracted from the cells using the RNeasy Mini Kit (QIAGEN, Hilden, Germany), and cDNAs were synthesized from 1 μg of total RNA with oligo dT primers using the Omniscript RT kit (QIAGEN). Quantitative RT-PCR was performed using ABI PRISM 7000 (Applied Biosystems, Foster City, CA, USA) according to the manufacturer's instructions. The PCR primers used are as follows:

